

Anion-Controlled Assembly of Silver(I) Complexes of Multiring Heterocyclic Ligands: A Structural and Photophysical Study

Nabanita Kundu,[†] Anandalok Audhya,[†] Sk Md Towsif Abtab,[†] Sanjib Ghosh,[‡] Edward R. T. Tiekink,^{*,§,¶} and Muktimoy Chaudhury^{*,†}

[†]Department of Inorganic Chemistry, Indian Association for the Cultivation of Science, Kolkata 700 032, India, [‡]Department of Chemistry, Presidency College, Kolkata 700 073, India, [§]School of Materials Science and Engineering, Nanyang Technological University, Singapore 639798, and [¶]Department of Chemistry, University of Malaya, 50603 Kuala Lumpur, Malaysia

Received October 16, 2009; Revised Manuscript Received December 18, 2009

ABSTRACT: Four multiring heterocyclic ligands with benzimidazole (L^1 and L^3) and benzothiazole nuclei (L^2 and L^4) are reported. Their silver(I) complexes involving a variety of anions (both organic and inorganic) have been prepared by the process of self-assembly and structurally characterized by single-crystal X-ray diffraction analyses. Discrete metalocyclic complexes $[Ag(L^3)(X)]_2$ ($X = NO_3^-$, **3a**; *cis*-HOOCCH=CHCOO⁻, **3b**; $0.5SiF_6^{2-}$, **3c**) and $[Ag(L^4)(Y)]_2$ ($Y = NO_3^-$, **4a**; $CF_3SO_3^-$, **4b**) have been formed with the ligands L^3 and L^4 , respectively, where the pyridine nitrogen atom N1 is in the 3-position as against the coordination polymers $[Ag(L^1)(H_2O)(NO_3)]_n$, **1a**, $[Ag(L^1)(CF_3COO)]_n$, **1b** and $\{2[Ag(L^2)_2(ClO_4)] \cdot 0.5 \cdot C_2H_5OH\}_n$, **2a**, and $[Ag(L^2)_2(cis-HOOCCH=CHCOO)]_n$, **2b**, with the ligands L^1 and L^2 , respectively, in which the N1 atom occupies the 4-position in the pyridine ring. In addition to the primary ligands (L^1 – L^4), the counteranions also have a dominant influence on the overall structures of these compounds. Secondary bonding interactions, namely, hydrogen bonding, $\pi \cdots \pi$ -stacking, and C–H \cdots π interactions, are also proven effective in shaping the dimensionalities of the solid state structures. Thus, a zigzag chain structure of **1a** mediated by a nitrate anion generates a more complicated double layer structure in **1b** where trifluoroacetate has replaced nitrate as the counterion. Discrete 12-membered metalocycles in **3a**–**3c** generate 2-D arrays of flat (**3a**) and undulating topologies (**3b** and **3c**), depending upon the type of their associated anions. Metalocycles **4a** and **4b** have less complicated structures compared to those of **3a**–**3c** because of the replacement of NH by S in the heterocyclic ring, thereby reducing the hydrogen-bonding potential in the primary ligand in going from L^3 to L^4 . In the solid state, the complexes show enhanced phosphorescence at 77 K with triplet lifetime in the range of 0.5–0.8 s, much shorter than those for the free ligands (2.3–3.3 s) because of increased spin–orbit coupling introduced by the coordinated Ag^+ ion. This heavy-atom effect also has a causative influence in shortening the fluorescence lifetimes of these compounds.

Introduction

Crystal engineering of supramolecular architectures involving metalloorganic frameworks (MOFs) as building blocks is a rapidly developing area of research in contemporary coordination chemistry because of their intrinsic aesthetic appeal,¹ as well as for many of their fascinating properties, both realized and potential, in the domains of catalysis, nonlinear optics, magnetism, microelectronics, exchange and storage materials, etc.² The observed properties are very much influenced by subtle changes in the network structure of the polymeric entities and the development of synthetic strategies to generate the desired product with a predefined property is a long-term challenge. Numerous routes have been investigated in recent times, some are controlled by the formation of conventional bonds and others by supramolecular contacts such as hydrogen bonding, π – π -stacking and X–H \cdots π ($X = O, N, C$) interactions, etc.^{3–9}

Since the pioneering work of Thompson and Forrest¹⁰ regarding the application of phosphorescent metal–organic luminophores as emitting materials in solid-state organic light-emitting devices (OLEDs), major emphasis is now placed on the development of new MOFs as emitters for OLEDs. Because of mixing of the singlet and triplet states in heavy metal phosphorescent complexes through efficient

spin–orbit coupling, the luminous efficiency of OLEDs may potentially be improved to a large extent.¹¹ Many such compounds with interesting phosphorescence properties have also found applications in light emitting electrochemical cells (LEC)^{12–16} and in phosphorescence based photodynamic therapy.¹⁷ Ionic complexes are particularly promising for LEC device applications since they facilitate electronic charge injection into the light emitting film.^{16,18,19} High phosphorescence intensity of the emitters with sharp color in the blue, green, and red regions enables high efficiency in LEC. Coordination polymers are widely regarded as promising materials for many optoelectronic device applications because of their higher thermal stability, superior quantum efficiency, brightness, and insolubility in polar and nonpolar solvents.^{20–23} In addition, complexation of organic chromophores to the metal atoms and the presence of several supramolecular interactions induced by anions, solvents, metal–metal interactions, etc., help in tuning their emission wavelengths, making these materials attractive for both fundamental research and practical applications.

Silver complexes have attracted enormous attention over the years with the observation of a large variety of coordination architectures, structural variability correlated with disparate anions or solvent, and fascinating luminescence properties;²⁴ several reviews are available.²⁵ Examples of highlights from the very recent literature include a direct white-light emitting silver-based MOF,^{26a} anion-dependent

*Authors to whom correspondence should be addressed. E-mail: Edward.Tiekink@gmail.com (E.R.T.T.); icmc@iacs.res.in (M.C.).

mesomorphism,^{26b} and conformational polymorphism in helical coordination polymers,^{26c} and variable self-assembly mechanisms and coordination geometries in architectures based on noncovalent interactions.^{26d–26f} Such a rich and diverse chemistry, often leading to aesthetically pleasing structural motifs in addition to materials with potentially useful properties, underscores the intense contemporary interest in the supramolecular chemistry of silver and offers challenges for their systematic and controlled assembly.

Herein, we report the synthesis and photophysical properties of some supramolecular cationic silver(I) complexes (**1a**, **1b**, **2a**, **2b**, **3a–3c**, **4a**, and **4b**) and describe a strategy to tune the phosphorescence wavelength and enhance their emission intensity. These have been achieved by (i) varying the counteranions of these cationic complexes, (ii) changing the non-coordinating heteroatom (S in place of NH), and (iii) changing the relative positions of the coordinating atoms in a series of closely related ligands (L^1 – L^4). The ease of synthesis of these heterocyclic rigid multiring ligands and their metal complexes readily allows structural modification for the optimization of their photophysical properties.

Experimental Section

Materials. Silver maleate was prepared by combining an equivalent of silver carbonate with an aqueous solution of maleic acid. Pyridine-4-carboxaldehyde, pyridine-3-carboxaldehyde, 2-aminothiophenol, and silver trifluoroacetate were purchased from Aldrich. All other reagents were commercially available and used as received. Solvents were reagent grade, dried by standard methods²⁷ and distilled under nitrogen prior to use.

Preparation of Ligands. Ligands L^1 – L^4 were prepared following a general procedure. The synthesis of 2-(pyridin-4-yl)-1H-benzodimidazole (L^1) is described as an archetype.

2-(Pyridin-4-yl)-1H-benzodimidazole (L^1). To a stirred solution of *o*-phenylenediamine (1.08 g, 10 mmol) in methanol (25 mL) was added an equimolar amount of pyridine-4-carboxaldehyde (1.07 g) in the same solvent (10 mL). The solution was stirred for 30 min and then evaporated to dryness under reduced pressure. The crude product was recrystallized from ethyl acetate to get a yellow-brown product. Yield: (80%). mp: 224 °C. Anal. Calcd for $C_{12}H_9N_3$: C, 73.83; H, 4.64; N, 21.52. Found: C, 73.64; H, 4.58; N, 21.59%. IR (KBr pellet, cm^{-1}): 3467br, 3072, 1610, 1436, 1000, 829, 742, 692. UV–vis (CH_3OH) [λ_{max} , nm (ϵ , $mol^{-1} cm^2$): 311 (25 100), 243 (8800), 208 (22 200)]. 1H NMR (300 MHz, CD_3OD , 293 K, δ/ppm): 8.72 (d, 2H, $J = 6.0$ Hz), 8.08 (d, 2H, $J = 6.0$ Hz), 7.66 (s, 2H), 7.33 (m, 2H).

2-(Pyridin-4-yl)benzo[d]thiazole (L^2). This compound was prepared using 2-aminothiophenol and pyridine-4-carboxaldehyde following an identical procedure as mentioned above for L^1 . The compound was recrystallized from methanol as a yellow-brown product. Yield: 89%. mp: 130 °C. Anal. Calcd for $C_{12}H_8N_2S$: C, 67.90; H, 3.79; N, 13.19. Found: C, 68.02; H, 3.70; N, 13.32%. IR (KBr pellet, cm^{-1}): 3483br, 1593, 1475, 1407, 977, 823, 704. UV–vis (CH_3OH) [λ_{max} , nm (ϵ , $mol^{-1} cm^2$): 302 (18 100), 255 (7100), 217 (23 800), 205 (28 500)]. 1H NMR (300 MHz, $CDCl_3$, 293 K, δ/ppm): 8.77 (d, 2H, $J = 5.8$ Hz), 8.13 (d, 1H, $J = 8.3$ Hz), 7.95 (m, 3H), 7.55 (m, 1H), 7.46 (m, 1H).

2-(Pyridin-3-yl)-1H-benzodimidazole (L^3). This compound was prepared as described for L^1 , but using pyridine-3-carboxaldehyde. The product was recrystallized from methanol as an off-white solid. Yield: 82%. mp: 246 °C. Anal. Calcd for $C_{12}H_9N_3$: C, 73.83; H, 4.64; N, 21.52. Found: C, 73.44; H, 4.52; N, 21.85%. IR (KBr pellet, cm^{-1}): 3043br, 2678, 1623, 1575, 1448, 1429, 1317, 962, 744, 711, 702. UV–vis (CH_3OH) [λ_{max} , nm (ϵ , $mol^{-1} cm^2$): 305 (17 000), 240 (8500)]. 1H NMR (300 MHz, CD_3OD , 293 K, δ/ppm): 9.26 (bs, 1H), 8.66 (d, 1H, $J = 1.2$ Hz), 8.48 (m, 1H), 7.62 (m, 3H), 7.30 (dd, 2H, $J = 3.1, 6.1$ Hz).

2-(Pyridin-3-yl)benzo[d]thiazole (L^4). This compound was prepared using 2-aminothiophenol and pyridine-3-carboxaldehyde

following the procedure described for L^1 . The compound was recrystallized from methanol as an off-white solid. Yield: 90%. mp: 125 °C. Anal. Calcd for $C_{12}H_8N_2S$: C, 67.90; H, 3.79; N, 13.19. Found: C, 67.58; H, 3.87; N, 13.31%. IR (KBr pellet, cm^{-1}): 3481br, 3053, 1608, 1460, 1427, 1309, 964, 765, 704. UV–vis (CH_3OH) [λ_{max} , nm (ϵ , $mol^{-1} cm^2$): 299 (16 700), 248 (7100), 224 (19 000)]. 1H NMR (300 MHz, $CDCl_3$, 293 K, δ/ppm): 9.29 (d, 1H, $J = 2.1$ Hz), 8.71 (dd, 1H, $J = 1.4, 4.8$ Hz), 8.37 (m, 1H), 8.10 (d, 1H, $J = 8.1$ Hz), 7.92 (d, 1H, $J = 7.7$ Hz), 7.52 (m, 1H), 7.45–7.39 (m, 2H).

Preparation of Complexes. [$Ag(L^1)(H_2O)(NO_3)_n$] (**1a**). A methanolic solution (5 mL) of L^1 (19.5 mg, 0.1 mmol) was carefully layered on to a solution of silver nitrate (16.9 mg, 0.1 mmol) in water (25 mL). Diffusion between the two layers over a period of four days produced brown crystals. Yield: 34 mg (89%). Anal. Calcd for $C_{12}H_{11}AgN_4O_4$: C, 37.62; H, 2.89; N, 14.62. Found: C, 37.76; H, 3.01; N, 14.52%. IR (KBr pellet, cm^{-1}): 3215br, 1610, 1429, 1383, 1220, 831, 742, 690.

[$Ag(L^1)(CF_3COO)_n$] (**1b**). This compound was prepared as a brown crystalline solid following an identical procedure as described for **1a** but using silver trifluoroacetate. Yield: 84%. Anal. Calcd for $C_{14}H_9AgF_3N_3O_2$: C, 40.41; H, 2.18; N, 10.09. Found: C, 40.22; H, 2.12; N, 10.21%. IR (KBr pellet, cm^{-1}): 3421br, 3099, 1681, 1662, 1612, 1436, 1205, 1124, 837, 744.

{ $2[Ag(L^2)(ClO_4)] \cdot 0.5C_2H_5OH$ }_n (**2a**). An ethanolic solution (5 mL) of L^2 (21.2 mg, 0.1 mmol) was carefully poured on to a solution of silver perchlorate monohydrate (22.5 mg, 0.1 mmol) in water (10 mL), forming two distinct layers. Diffusion between these two layers over a period of two days produced a light-yellow crystalline compound. Yield: 51.47 mg (80%). Anal. Calcd for $C_{49}H_{35}Ag_2Cl_2N_8O_{8.5}S_4$: C, 45.73; H, 2.74; N, 8.70. Found: C, 45.81; H, 2.62; N, 8.76%. IR (KBr pellet, cm^{-1}): 3494br, 3056, 1606, 1552, 1477, 1431, 1413 1141, 1110, 1087, 759, 707, 624.

[$Ag(L^2)_2(cis-HOOCCH=CHCOO)_n$] (**2b**). This compound was prepared following the procedure described for **2a** using a methanolic solution of L^2 and an aqueous solution of silver maleate. Light-yellow crystals were obtained within three days. Yield: 84%. Anal. Calcd for $C_{28}H_{19}AgN_4O_8S_2$: C, 51.94; H, 2.95; N, 8.65. Found: C, 51.56; H, 2.88; N, 8.56%. IR (KBr pellet, cm^{-1}): 3436br, 3053, 2885, 1606, 1583, 1475, 1468, 1429, 1350, 1186, 979, 761, 709, 551.

[$Ag(L^3)(NO_3)_2$] (**3a**). A solution of L^3 (19.5 mg, 0.1 mmol) in methanol (5 mL) was allowed to diffuse slowly on to an aqueous solution (10 mL) of silver nitrate (17 mg, 0.1 mmol). Within a period of five days a white crystalline compound was obtained. Yield: 29.2 mg (80%). Anal. Calcd for $C_{24}H_{18}Ag_2N_8O_6$: C, 39.47; H, 2.48; N, 15.34. Found: C, 40.00; H, 2.51; N, 15.42%. IR (KBr pellet, cm^{-1}): 3460br, 3049, 1448, 1382, 1313, 746, 698, 671.

[$Ag(L^3)(cis-HOOCCH=CHCOO)_2$] (**3b**). This compound was prepared as a yellow crystalline solid as described for **3a** but using silver maleate. Yield: 78%. Anal. Calcd for $C_{32}H_{24}Ag_2N_6O_8$: C, 45.95; H, 2.89; N, 10.04. Found: C, 46.20; H, 2.93; N, 10.30%. IR (KBr pellet, cm^{-1}): 3431br, 3055, 2883, 1608, 1577, 1481, 1448, 1417, 1379, 1353, 968, 707, 694.

[$Ag(L^3)(SiF_6)_{0.5}2$] (**3c**). This compound was prepared as a yellow crystalline solid following an identical procedure as described for **3a** but using silver hexafluorosilicate. Yield: 81%. Anal. Calcd for $C_{24}H_{18}Ag_2F_6N_6Si$: C, 38.52; H, 2.42; N, 11.23. Found: C, 39.01; H, 2.42; N, 11.01%. IR (KBr pellet, cm^{-1}): 3452br, 3053, 2927, 1450, 952, 750, 640.

[$Ag(L^4)(NO_3)_2$] (**4a**). A solution of the ligand L^4 (21.2 mg, 0.1 mmol) in methanol (5 mL) was carefully layered over a solution of silver nitrate (17 mg, 0.1 mmol) in water (10 mL). Diffusion between the two solutions over a period of three days produced light-yellow crystals. Yield: 31.7 mg (83%). Anal. Calcd for $C_{24}H_{16}Ag_2N_6O_6S_2$: C, 37.71; H, 2.10; N, 10.99. Found: C, 37.81; H, 2.15; N, 11.12%. IR (KBr pellet, cm^{-1}): 3483br, 3051, 1461, 1429, 1382, 964, 765, 702.

[$Ag(L^4)(CF_3SO_3)_2$] (**4b**). This compound was prepared as a light yellow crystalline solid following an identical procedure as described for **4a** using silver trifluoromethanesulfonate as a replacement for silver nitrate. Yield: 80%. Anal. Calcd for $C_{26}H_{16}Ag_2F_6N_4O_6S_4$: C, 33.27; H, 1.72; N, 5.97. Found: C, 33.36; H, 1.71; N, 6.18%. IR (KBr pellet, cm^{-1}): 3431br, 3083, 1596, 1429, 1271, 1249, 1166, 1049, 1024, 763, 698, 657, 628.

Table 1. Crystallographic Parameters and Refinement Details for **1a**, **1b**, **2a** and **2b**

parameter	1a	1b	2a	2b
formula	C ₁₂ H ₁₁ AgN ₄ O ₄	C ₁₄ H ₉ AgF ₃ N ₃ O ₂	C ₄₉ H ₃₅ Ag ₂ Cl ₂ N ₈ O _{8.5} S ₄	C ₂₈ H ₁₉ AgN ₄ O ₄ S ₂
fw	383.12	416.11	1286.77	647.46
cryst syst	orthorhombic	monoclinic	monoclinic	triclinic
space group	<i>Aba2</i>	<i>C2/c</i>	<i>P2₁/c</i>	<i>P$\bar{1}$</i>
<i>a</i> , Å	18.0934(12)	20.362(4)	11.7893(5)	5.280(4)
<i>b</i> , Å	12.9305(9)	10.759(2)	16.9090(7)	7.4235(5)
<i>c</i> , Å	10.9566(8)	14.713(3)	24.3902(11)	28.6613(17)
α , deg	90	90	90	87.738(1)
β , deg	90	119.614(4)	94.909(1)	85.342(1)
γ , deg	90	90	90	83.904(1)
<i>V</i> , Å ³	2563.4(3)	2802.2(10)	4844.2(4)	1228.33(14)
<i>Z</i>	8	8	4	2
μ , cm ⁻¹	1.596	1.486	1.158	1.037
<i>D_x</i> , g cm ⁻³	1.985	1.973	1.764	1.751
no. unique reflns	2194	2004	11123	5634
no obsd reflns with <i>I</i> > 2 σ (<i>I</i>)	1849	1680	8295	5082
<i>R</i> (obsd data)	0.031	0.029	0.058	0.042
<i>a, b</i> in weighting scheme	0.035, 0	0.040, 2.129	0.064, 9.599	0.065, 0.154
<i>R_w</i> (all data)	0.066	0.071	0.160	0.114
CCDC No.	666481	666482	666483	666484

Caution! Perchlorate salts of metal complexes containing organic ligands are potentially explosive²⁸ and should be handled in small quantities with sufficient care.

Physical Measurements. Microanalyses (for C, H and N) were performed at IACS using a Perkin-Elmer model 2400 Series II elemental analyzer. ¹H NMR, IR, and electronic spectra were recorded using instruments as described elsewhere.²⁹ The steady state fluorescence measurements were carried out in a Hitachi F-7000 spectrofluorimeter (equipped with a 150 W xenon lamp) using a 1 cm path length quartz cuvette. All the fluorescence measurements at 77 K were taken by exciting the samples at 243 and 330 nm using 5 nm band-passes for excitation and emission. Emission studies at 77 K were conducted using a Dewar system having a 5 mm outside diameter quartz tube; freezing of the samples at 77 K was carried out at the same rate for all the samples. Triplet state emissions were measured in a Hitachi F-7000 spectrofluorimeter equipped with phosphorescence accessories at 77 K. The samples were excited using a 10 nm band-pass, and the emission band-pass was 1.5 nm.

Singlet state time-resolved emission studies were carried out in a Time Master Fluorimeter from Photon Technology International (PTI), U.S.A. The system measures the fluorescence lifetime using PTI's patented strobe technique and gated detection. The software Felix 32 controls all acquisition modes and data analysis of the Time Master system.³⁰ The sample was excited using a thyratron gated nitrogen flash lamp fwhm 1.2 ns that is capable of measuring fluorescence time-resolved acquisition at flash rate of 25 kHz. Lamp profiles were measured at the excitation wavelength using slits with a band-pass of 3 nm using Ludox as the scatterer. The decay parameters were recovered using a nonlinear iterative fitting procedure based on the Marquardt algorithm. The quality of the fit was assessed over the entire decay, including the rising edge, and tested with a plot of weighted residuals and other statistical parameters, for example, the reduced χ^2 ratio.³⁰ The phosphorescence lifetime was measured using a Hitachi F-4010 spectrofluorimeter equipped with a phosphorescence accessory.

X-ray Crystallography. Diffraction grade crystals in each case were collected from the reaction pot for crystal structure analysis. Intensity data were measured at 223(2) K on a Bruker SMART CCD diffractometer employing Mo K α radiation. Data processing and empirical absorption corrections were accomplished with the programs SAINT^{31a} and SADABS,^{31b} respectively. The structures were solved by heavy-atom methods^{31c} and refinements (anisotropic displacement parameters, hydrogen atoms in the riding model approximation and a weighting scheme of the form $w = 1/[\sigma^2(F_o^2) + aP^2 + bP]$ for $P = (F_o^2 + 2F_c^2)/3$) were on F^2 .^{31d} Data sets were truncated so that $2\theta_{\max}$ was 55.0°. However, in the cases of **1b** and **3c**, irretrievable processing errors resulted in the data sets being truncated at $2\theta_{\max} = 46.4^\circ$. Although each of these data sets is incomplete in terms of the range of 2θ used in the refinement, the molecular structures present no unusual features and have been

determined unambiguously. The structure of **1a** was refined as a racemic twin. The crystallographic asymmetric unit of **2a** comprises a pair of $[\text{Ag}(\text{L}^2)_2]^+$ complex cations, two perchlorate anions and half a solvent ethanol molecule of crystallization. Disorder in each of the cations was detected in terms of interchange of the sulfur and nitrogen atoms. Fractional refinement gave site occupancies for the S1–S4 atoms of 0.651(5), 0.858(7), 0.913(6), and 0.780(5), respectively. High thermal motion was also detected for the perchlorate anions in **2a** but multiple sites could not be resolved. Crystallographic data and final refinement details are given in Tables 1 and 2. Figures 1, 3, 5a, 6, and 8 were drawn with ORTEP-II^{31e} at 50% probability level (35% for **1a**, **1b**, **4a**, and **4b**) and the remaining figures were drawn with the DIAMOND program.^{31f} Data manipulation and analysis were accomplished with teXsan^{31g} and PLATON.^{31h}

Results and Discussion

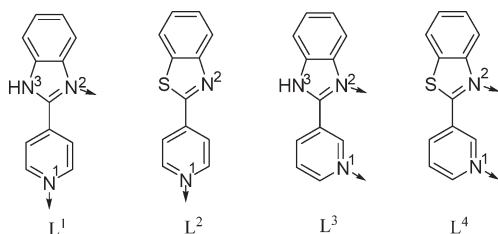
Syntheses. A high yield (80–90%) protocol has been developed for the synthesis of multiring rigid heterocyclic ligands (L¹–L⁴) involving 2-pyridyl substitutions in benzimidazole and benzothiazole rings. Such molecules are known to have various therapeutic applications³² and show enormous potential as pharmacophores in contemporary drug discovery research.³³ The neutral ligands with the benzimidazole appendage, that is, L¹ and L³, Chart 1, have three different nitrogen atoms of which only N1 and N2 are capable of coordination to Ag atoms, thus making these to coordinate as potentially ditopic ligands. The tertiary nitrogen N3 on the other hand can only participate in supramolecular aggregation through hydrogen bonding. Replacement of this tertiary nitrogen NH in L¹ and L³ by sulfur generates the ligands L² and L⁴, respectively, containing a benzothiazole nucleus. Between the latter, L⁴ is ditopic while L² coordinates Ag atom in a monotopic fashion. Silver being a soft metal atom, is expected to be coordinated by the sulfur atom^{9k,9n} in the complexes with L² and L⁴. However, this does not happen in the systems investigated here as in both the cases sulfur, being part of a five-membered thiazole ring, engages one of its electron lone-pairs to fulfill the aromatic sextet of the ring and subsequently becomes too weakly basic to participate in metal coordination.

Coordination polymers of silver(I) are remarkably susceptible to the influence of the ligands, anion functionality and the solvent type used in the syntheses.^{2c,25} Complexes **1a**, **1b**, **2a**, **2b**, **3a–3c**, **4a**, and **4b** have been synthesized by the reactions between the ligands L¹–L⁴ and the metal salts AgX

Table 2. Crystallographic Parameters and Refinement Details for 3a–3c, 4a, and 4b

parameter	3a	3b	3c	4a	4b
formula	C ₂₄ H ₁₈ Ag ₂ N ₈ O ₆	C ₃₂ H ₂₄ Ag ₂ N ₆ O ₈	C ₂₄ H ₁₈ Ag ₂ F ₆ N ₆ Si	C ₁₃ H ₈ AgN ₃ O ₃ S	C ₁₃ H ₈ AgF ₃ N ₂ O ₃ S ₂
fw	730.20	836.32	748.27	382.15	469.20
cryst syst	triclinic	monoclinic	monoclinic	triclinic	triclinic
space group	$P\bar{1}$	$P2_1/n$	$C2/c$	$P\bar{1}$	$P\bar{1}$
<i>a</i> , Å	8.2886(7)	4.8547(3)	15.924(2)	8.6754(11)	8.0905(4)
<i>b</i> , Å	9.0739(7)	21.3116(13)	11.5960(17)	8.8529(11)	9.9052(5)
<i>c</i> , Å	9.8794(8)	14.3407(8)	12.9422(19)	9.5078(11)	10.4672(6)
α , deg	106.184(2)	90	90	102.345(3)	109.183(1)
β , deg	96.569(2)	96.1150(10)	93.207(3)	114.366(2)	101.972(1)
γ , deg	116.873(2)	90	90	102.287(3)	97.667(1)
<i>V</i> , Å ³	610.95(9)	1475.27(15)	2386.1(6)	611.49(13)	756.34(7)
<i>Z</i>	1	2	4	2	2
μ , cm ⁻¹	1.663	1.394	1.768	1.829	1.658
<i>D_x</i> , g cm ⁻³	1.985	1.883	2.083	2.075	2.060
no. reflns	2771	3401	1713	2784	3461
no obsd reflns with <i>I</i> > 2 σ (<i>I</i>)	2522	2948	1600	2315	3219
<i>R</i> (obsd data)	0.033	0.033	0.022	0.033	0.028
<i>a</i> , <i>b</i> in weighting scheme	0.053, 0.328	0.046, 0.298	0.034, 3.259	0.045, 0	0.036, 0.521
<i>R_w</i> (all data)	0.097	0.085	0.057	0.082	0.070
CCDC No.	666485	666486	666487	666488	666489

Chart 1



(X = NO₃⁻, ClO₄⁻, CF₃SO₃⁻, CF₃CO₂⁻, *cis*-HO₂CCH=CHCO₂⁻, and SiF₆²⁻) in a methanol–water medium. For compound **2a**, ethanol was used instead of methanol to aid crystallization of the compound. Variation of the Ag(I)/L ratio practically has no influence on the composition of the products despite it being known that coordination numbers from two to six are all possible for silver(I).³⁴ The new compounds are all coordination/supramolecular polymers with diversified structural features because of the flexible coordination behavior of silver(I), hydrogen bonding by the coordinated ligands (L¹–L⁴), and secondary bonding interactions from the anions. These are all sparingly soluble compounds in common organic solvents and show immense light-stability in the solid state.

IR spectra of the complexes display all the pertinent bands of the coordinated heterocyclic ligands. In addition, complexes **1a**, **3a**, and **4a** display a strong band at ~1380 cm⁻¹ because of the presence of NO₃⁻ anion. For **1b**, four strong bands in the 1685–1120 cm⁻¹ region appear as a signature for the CF₃CO₂⁻ anion.⁶ The appearance of strong and medium intensity bands at 1087 and 624 cm⁻¹, respectively, confirms the presence of ionic perchlorate in **2a**.³⁵ In compounds **2b** and **3b**, four carboxylate stretchings are observed, two in the form of strong bands in the 1610–1570 cm⁻¹ region and two as medium intensity broad bands in the 1380–1350 cm⁻¹ range. These are the result of the antisymmetric $\nu_a(\text{COO}^-)$ and symmetric $\nu_s(\text{COO}^-)$ vibrations, respectively, originating from two different types of carboxylates present in those compounds, one of which is protonated, while the other is in the deprotonated form.³⁵ The IR spectrum of **4b** displays three bands at 1249, 1166, and 1024 cm⁻¹, characteristic of the CF₃SO₃⁻ anion.⁶ A strong, albeit broad, feature at 750 cm⁻¹ provides a signature for the SiF₆²⁻ anion in **3c**.

Description of Crystal Structures. Full structural characterization of the complexes **1a**, **1b**, **2a**, **2b**, **3a–3c**, **4a**, and **4b** was afforded by single crystal X-ray crystallography. The relevant metrical parameters are displayed in Table 3. The crystallographic asymmetric unit of [Ag(L¹)(OH₂)(NO₃)_{*n*}] (**1a**) comprises a [Ag(L¹)]⁺ cation, a weakly coordinated water molecule and a nitrate anion as displayed in Figure 1A. The structure of **1a** is oligomeric with the Ag atom being coordinated by the imine-N2 atom (2.162(3) Å) and a symmetry related pyridine-N1ⁱ atom (2.214(4) Å; (i) 11/2 - x, y, -1/2 + z) that define an approximately linear coordination geometry, 150.9(1)°. Distortions from the ideal are related to the loose contact formed between the Ag atom and the water molecule of crystallization (2.582(4) Å), and if considered to form a significant interaction, the coordination geometry is approximately T-shaped with O4–Ag–N2, N1ⁱ angles of 114.5(1) and 89.6(1)°, respectively. The topology of the resultant oligomer is a zigzag chain aligned along the *c*-axis, and this is stabilized by internal O_{water}–H···O_{nitrate} and N_{amine}–H···O_{nitrate} hydrogen bonds,³⁶ shown in Figure 2A. The chains pack alongside each other in the *ac*-plane, being connected by a number of weak C–H···O_{nitrate} contacts. The second hydrogen atom of each water molecule is disposed to one side of the *ac*-plane and serves to connect layers related by 2-fold symmetry via by O_{water}–H···O_{nitrate} interactions to form a double layer as highlighted in Figure 2B. Interactions of the $\pi\cdots\pi$ type, formed between the five-membered rings, serve to consolidate the double layer and the primary interactions between the double layers are of the type C–H···O.³⁶ The coordination geometry about the Ag atom in [Ag(L¹)(O₂CCF₃)_{*n*}] (**1b**) is distinct to that just described (Figure 1B), with Ag–N2, N1ⁱ bond distances of 2.192(3) and 2.257(3) Å, respectively. These are each longer than the comparative bond in **1a** and subtend an angle of 145.1(1)° at the Ag atom; *i* = 11/2 - x, 1/2 + y, 21/2 - z. The variation in structure is traced to the coordination mode of the CF₃CO₂⁻ anion, which is loosely associated to the Ag atom (Ag···O1 = 2.520(3) Å) but at the same time forms a second interaction, also via the O1 atom, to a symmetry related Ag atom, Ag···O1ⁱⁱ = 2.559(3) Å (*ii* = 11/2 - x, 11/2 - y, 2 - z). This has the dual result that the Ag atom is pseudotetrahedral as shown in Figure 2C, with a range of angles, excluding the aforementioned N2–Ag–N1ⁱ angle, of 76.9(1)° for O1–Ag–O1ⁱⁱ to 115.6(1)° for O1–Ag–N2, and that a binuclear [Ag₂(L¹)₄(O₂CCF₃)₂] aggregate ensues. This

Table 3. Selected Bond Lengths (Å) and Angles (deg) for 1a, 1b, 2a, 2b, 3a–3c, 4a, and 4b^a

1a					
Ag–N2	2.162(3)	Ag–N1 ⁱ	2.214(4)	Ag–O4	2.582(4)
N2–Ag–N1 ⁱ	150.9(1)	N2–Ag–O4	114.5(1)	N1 ⁱ –Ag–O4	89.6(1)
1b					
Ag–N2	2.192(3)	Ag–N1 ⁱ	2.257(3)	Ag–O1	2.520(3)
Ag–O1 ⁱⁱ	2.559(3)	O1–Ag–O1 ⁱⁱ	76.9(1)		
N2–Ag–N1 ⁱ	145.1(1)	N2–Ag–O1	115.6(1)	N1–Ag–O1 ⁱⁱ	91.1(1)
2a					
Ag1–N1	2.133(4)	Ag1–N3	2.140(4)	Ag2–N5	2.144(4)
Ag2–N7	2.144(4)	Ag2–Ag2 ⁱ	3.211(8)		
N1–Ag1–N3	178.9(2)	N5–Ag2–N7	173.4(2)		
2b					
Ag–N1	2.178(2)	Ag–N3	2.191(2)	Ag–O1	2.654(2)
Ag–O2 ⁱ	2.925(2)	Ag–O3 ⁱⁱ	3.045(3)		
N1–Ag–N3	174.7(8)				
3a					
Ag–N2	2.161(3)	Ag–N1	2.197(3)	Ag–O1	2.685(4)
Ag–O3	2.827(4)	Ag–O2 ⁱ	2.772(3)		
N2–Ag–N1	154.6(1)				
3b					
Ag–N2	2.190(2)	Ag–N1	2.224(2)	Ag–O1	2.501(2)
N2–Ag–N1	146.5(7)	N2–Ag–O1	116.4(8)	N1–Ag–O1	96.4(8)
3c					
Ag–N2	2.133(2)	Ag–N1	2.166(2)	Ag–F1	2.689(2)
Ag–F2 ⁱ	3.112(2)				
N2–Ag–N1	158.6(9)				
4a					
Ag–N2	2.219(3)	Ag–N1 ⁱ	2.225(3)	Ag–O1	2.565(3)
Ag–O2 ⁱⁱ	2.617(4)	Ag–O3 ⁱⁱⁱ	2.824(4)		
N2–Ag–N1 ⁱ	144.0(1)	N2–Ag–O1	106.3(9)	N1 ⁱ –Ag–O1	90.5(9)
4b					
Ag–N1 ⁱ	2.202(2)	Ag–N2	2.216(2)	Ag–O1	2.601(2)
Ag–O3 ⁱⁱ	2.612(2)	Ag–O2 ⁱⁱ	3.046(2)		
N1 ⁱ –Ag–N2	147.5(7)				

^a Symmetry operations. For **1a**: (i) $11/2 - x, y, -1/2 + z$. For **1b**: (i) $11/2 - x, 1/2 + y, 21/2 - z$; (ii) $11/2 - x, 11/2 - y, 2 - z$. For **2a**: (i) $2 - x, 1 - y, 1 - z$. For **2b**: (i) $-1 + x, y, z$; (ii) $x, 1 + y, z$. For **3a**: (i) $-x, 1 - y, 1 - z$. For **3c**: (i) $2 - x, 1 - y, -z$. For **4a** and **4b**: (i) $1 - x, 1 - y, 1 - z$; (ii) $-x, 1 - y, 1 - z$.

aggregate has four N-donor sites available for coordination to symmetry related Ag atoms and four N–H hydrogen bonding sites for the noncoordinating O2 atoms derived from CF₃CO₂[−] anions, and their participation in coordination/hydrogen bonding, respectively, leads to a 2-D array that stacks along the *b*-axis.³⁶ Within layers, zigzag chains, as found for **1a**, may be discerned but in this case alternating pivots in the chain, occupied by Ag atoms, are bridged to neighboring Ag atoms so that a double chain is formed with trifluoromethyl groups directed to the exterior of the layers and face each other in the stacking packing, displayed in Figure 2D.

Two independent [Ag(L²)₂] cations, two perchlorate anions, and a half occupied ethanol molecule of crystallization comprise the crystallographic asymmetric unit of 2[Ag(L²)₂(ClO₄)]·0.5EtOH (**2a**). The Ag atoms are linearly coordinated by two pyridine-N atoms (Ag1–N1, N3 = 2.133(4) and 2.140(4) Å, Ag2–N5, N7 = 2.144(4) and 2.144(4) Å) with N–Ag–N angles = 178.9(2) and 173.4(2)°, respectively. The key difference between the two cations is found in the relative orientations of the benzothiazole substituents so

that for the Ag1-cation, the sulfur atoms lie to one side of the molecule and in the Ag2-cation, they lie to opposite sides (Figure 3). On the basis of the relative disposition of the sulfur atoms, the isomers might be labeled syn and anti, respectively; minor disorder was noted in the occupancy of the S/N atoms (see Experimental Section) confirming that only a small energy difference exists between the conformations. The pyridine and thiazole residues are effectively coplanar in each case with the maximum twist between these residues seen in the C26/C27/C30/S3 torsion angle of $-169.7(4)^\circ$. A further difference in conformation within the cations is manifested in the dihedral angles between the pyridine residues of 89.2(2) and 7.0(2)° for the Ag1 and Ag2 cations, respectively, indicating orthogonal and coplanar conformations. Rather than being a simple structural oddity, these conformations have a profound influence on the crystal packing. The orthogonally shaped Ag1-cations aggregate head to tail, via $\pi \cdots \pi$ interactions,³⁷ to form twisted supramolecular chains aligned along the *b*-axis as displayed in Figure 4A. By contrast, centrosymmetrically related,

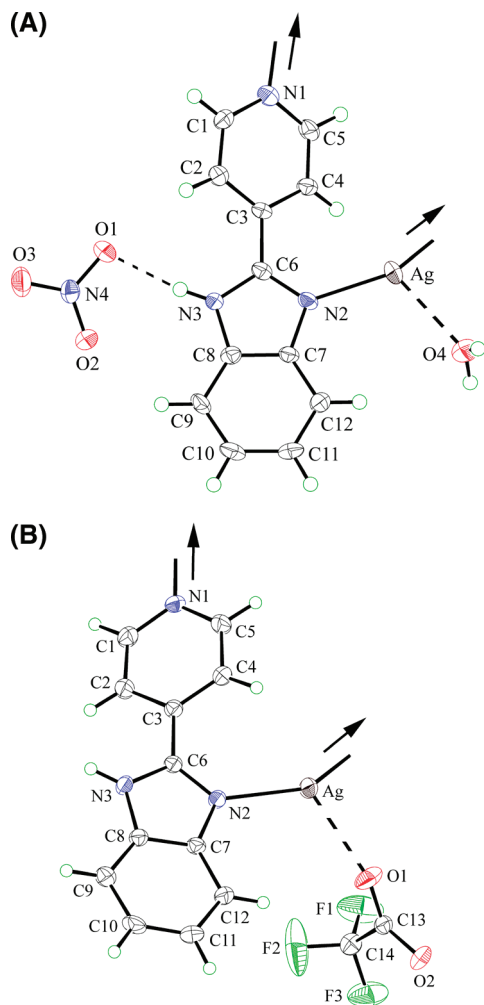


Figure 1. Crystallographic asymmetric unit showing atomic numbering schemes for (A) $[\text{Ag}(\text{L}^1)(\text{OH}_2)(\text{NO}_3)]_n$ (**1a**) and (B) $[\text{Ag}(\text{L}^1)(\text{O}_2\text{CCF}_3)]_n$ (**1b**). Intermolecular $\text{Ag}\cdots\text{O}$ interactions and $\text{N}-\text{H}\cdots\text{O}$ hydrogen bonding are shown as dashed lines.

approximately flat, Ag_2 -cations face each other being connected via argentophilic interactions ($\text{Ag}_2\cdots\text{Ag}_2^i = 3.211(8)$ Å), as well as via $\pi\cdots\pi$ interactions (Figure 4B):³⁷ (i) $2 - x, 1 - y, 1 - z$. The dimeric aggregates are interdigitated along the b -axis. There are additional $\pi\cdots\pi$ interactions operating between the supramolecular chains and columns of Ag_2 -cations,³⁷ and interspersed between these are channels occupied by the perchlorate anions and partially occupied ethanol molecules, with evidence for $\text{O}-\text{H}\cdots\text{O}$ hydrogen bonding between them (Figure 4C).³⁷ Changing the anion in (**2a**) to $\text{HO}_2\text{CC}(\text{H})=\text{C}(\text{H})\text{CO}_2^-$ leads to $[\text{Ag}(\text{L}^1)_2(\text{HO}_2\text{CC}(\text{H})=\text{C}(\text{H})\text{CO}_2)]_n$ (**2b**), featuring a planar conformation ($\text{Ag}-\text{N}1, \text{N}3 = 2.178(2)$ and $2.191(2)$ Å) and an “anti” disposition of the benzothiazole-S atoms (Figure 5A). The uninegative anion exhibits an internal $\text{O}-\text{H}\cdots\text{O}$ hydrogen bond³⁷ and forms a close $\text{Ag}\cdots\text{O}1$ contact of $2.654(2)$ Å, as well as weaker intermolecular $\text{Ag}\cdots\text{O}2^i$ and $\text{Ag}\cdots\text{O}3^{ii}$ contacts of $2.925(2)$ and $3.045(3)$ Å, respectively, (i) $-1 + x, y, z$ and (ii) $x, 1 + y, z$. In the crystal structure, stacks of cations associate along the b -axis via $\pi\cdots\pi$ interactions, the closest of which occurs between centrosymmetrically related benzothiazole rings,³⁷ and define channels in which reside the anions that form $\text{C}-\text{H}\cdots\text{O}$ contacts³⁷ with the cations, as indicated in Figure 5B.

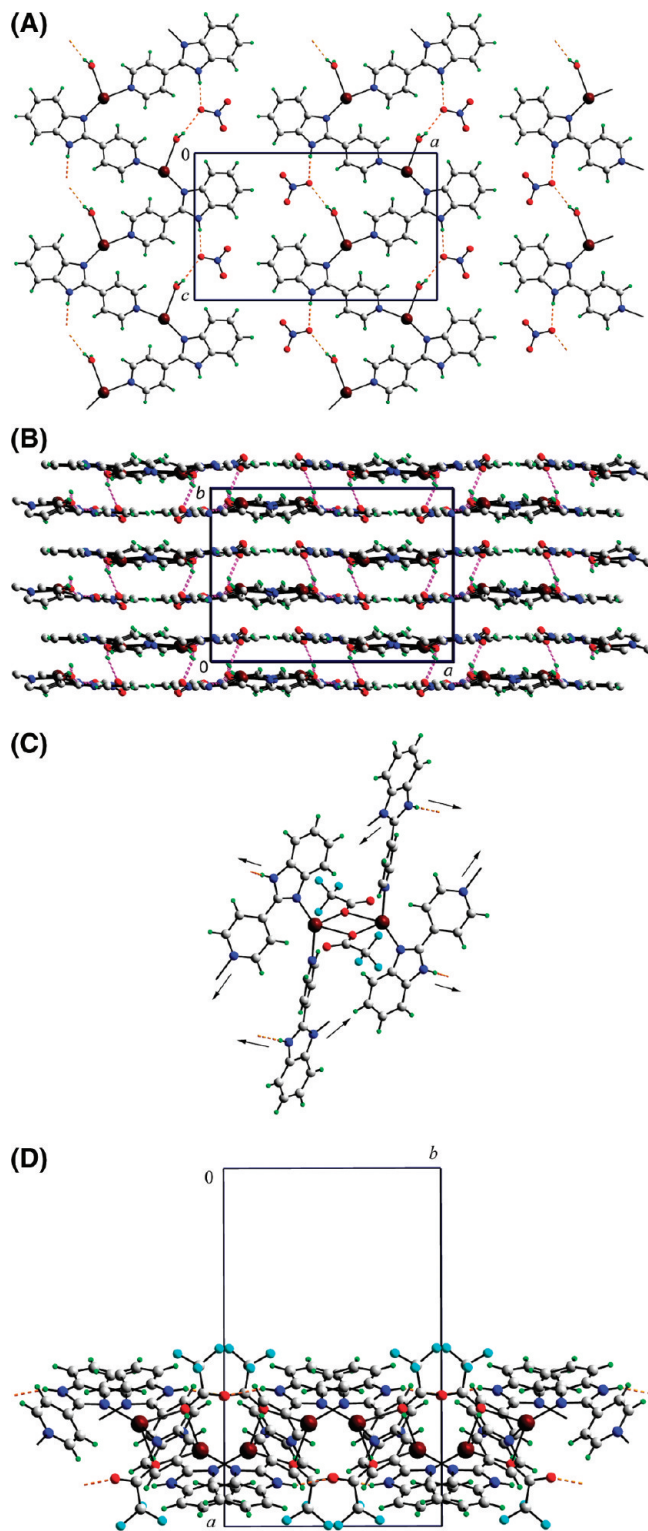


Figure 2. (A) Layer formation in the crystal structure of $[\text{Ag}(\text{L}^1)(\text{OH}_2)(\text{NO}_3)]_n$ (**1a**); $\text{O}-\text{H}\cdots\text{O}$ and $\text{N}-\text{H}\cdots\text{O}$ hydrogen bonds are shown as orange-dashed lines. (B) The water-bound H atoms not involved in hydrogen bonding within the layer shown in Figure 2A lie to the same side and interact via $\text{O}-\text{H}\cdots\text{O}$ hydrogen bonds (pink-dashed lines) with a layer related by 2-fold symmetry to form a double layer. The double layers stack along the b -axis. (C) Dimeric aggregate in $[\text{Ag}(\text{L}^1)(\text{O}_2\text{CCF}_3)]_n$ (**1b**) showing eight sites for supramolecular aggregation and (D) layer formation in the crystal structure. $\text{N}-\text{H}\cdots\text{O}$ hydrogen bonding is shown as orange-dashed lines.

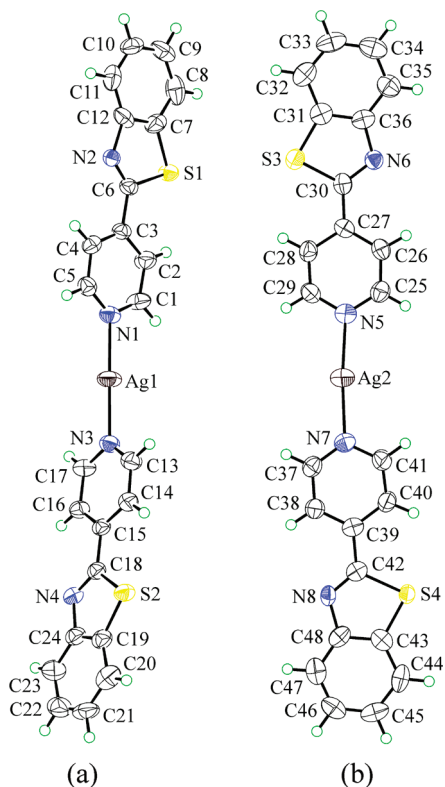


Figure 3. Molecular structures for the two independent cations in the crystallographic asymmetric unit of $2[\text{Ag}(\text{L}^2)(\text{ClO}_4)] \cdot 0.5\text{EtOH}$ (**2a**) showing atomic numbering schemes. For each molecule, only the major component of the disordered S/N atoms of each five-membered ring is shown for reasons of clarity (see Experimental Section).

A common feature of the next three structures to be described, that is, $[\text{Ag}(\text{L}^3)(\text{NO}_3)]_2$ (**3a**), $[\text{Ag}(\text{L}^3)(\text{HO}_2\text{CC}(\text{H})=\text{C}(\text{H})\text{CO}_2)]_2$ (**3b**), and $[\text{Ag}(\text{L}^3)(\text{SiF}_6)_{0.5}]_2$ (**3c**), is the formation of dimeric aggregates with essentially linear AgN_2 coordination geometries but with loosely associated anions as displayed in Figures 6A, 6B, and 6C, respectively. Oligomerization leading to metallocycles occurs in these structures owing to the relative disposition of the imine-N2 and 3-pyridine-N1 atoms. The sequence of $\text{Ag}-\text{N}_1$, N_2 bond distances is 2.197(3) and 2.161(3) Å, 2.224(2) and 2.190(2) Å and 2.166(2) and 2.133(2) Å, for **3a–3c**, respectively, that is, indicating an opposite trend in relative magnitudes of $\text{Ag}-\text{N}_{\text{imine}}$ and $\text{Ag}-\text{N}_{\text{pyridine}}$ bond distances compared to that seen in the structures of **1a** and **1b**. In **3a** and **3b**, the 12-membered rings are disposed about a center of inversion but in **3c**, the ring is disposed about a 2-fold axis. The different symmetry reflects the different conformations of the rings which adopt extended chair conformations in the cases of **3a** and **3b** but adopts a distinctly more concave arrangement in **3c**. The crystal packing in **3a–3c** is dominated by cation...anion interactions, as well as by $\text{N}-\text{H}\cdots\text{O}$, F hydrogen bonding.

In **3a**, a 2-D array is formed by the cross-linking of $\text{Ag}\cdots\text{O}$ interactions along the a -axis and $\text{N}-\text{H}\cdots\text{O}$ hydrogen bonding along the b -axis as displayed in Figure 7A. Each nitrate “chelates” one Ag atom ($\text{Ag}\cdots\text{O}1$, $\text{O}3 = 2.685(4)$ and $2.827(4)$ Å) and at the same time bridges a second Ag atom of a neighboring dimer ($\text{Ag}\cdots\text{O}2^1 = 2.772(3)$ Å for (i) $-x, 1-y, 1-z$). Orthogonal to these chains are $\text{N}-\text{H}\cdots\text{O}$ interactions.³⁸ The N–H atom is bifurcated but only the shortest contact is highlighted in Figure 7A. Interdigitation

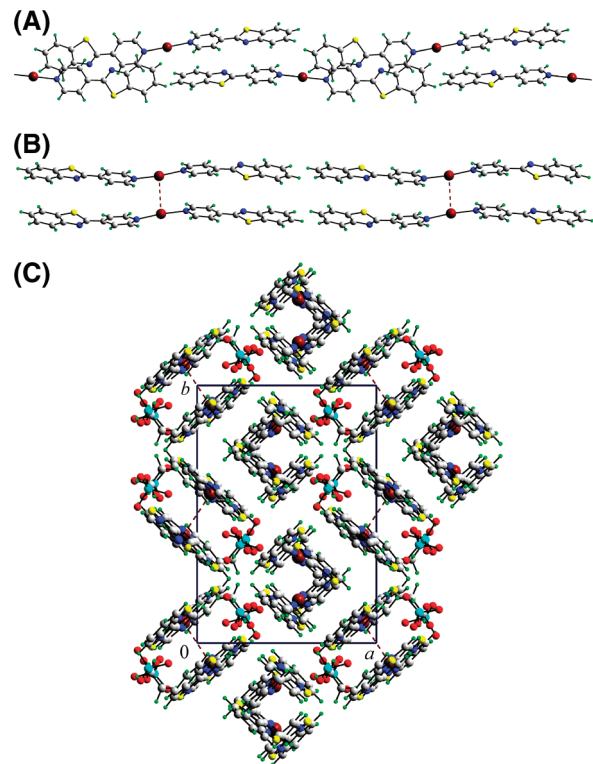


Figure 4. Views of the supramolecular association in $2[\text{Ag}(\text{L}^2)(\text{ClO}_4)] \cdot 0.5\text{EtOH}$ (**2a**): (A) supramolecular chain mediated by $\pi\cdots\pi$ interactions between Ag1-cations, (B) dimeric aggregates of Ag2-cations mediated by $\text{Ag}\cdots\text{Ag}$ (orange dashed lines) and $\pi\cdots\pi$ interactions; and (C) view of the unit cell contents down the c -axis.

between the layers along the c -axis allows for the formation of $\pi\cdots\pi$ interactions between the five-membered N2, N3, C6–C8, and aromatic C7–C12 rings, as well as $\text{C}-\text{H}\cdots\text{O}$ contacts.³⁸ 2-D arrays are also found in the crystal structure of **3b** (Figure 7B) but these have distinctive undulating topologies compared with the flat topology found in **3a**. The anion in **3b** features an intramolecular $\text{O}-\text{H}\cdots\text{O}$ bond³⁸ and forms only one primary interaction to the Ag atom, $\text{Ag}\cdots\text{O}1 = 2.501(2)$ Å, with the interaction reinforced by a charge-assisted $\text{C}-\text{H}\cdots\text{O}$ contact involving the O2 atom.³⁸ The carboxylate end of the anion forms a strong $\text{N}-\text{H}\cdots\text{O}$ hydrogen bond via the O4 atom to link a symmetry related dimer; these are complemented by $\text{C}-\text{H}\cdots\text{O}4$ contacts, not shown in Figure 7B.³⁸ Dimers, being surrounded by four anions, stack into columns primarily stabilized by $\pi\cdots\pi$ interactions between the five-membered N2, N3, C6–C8, and pyridine rings.³⁸ The undulating topology of this series features a dinegative SiF_6^{2-} anion and consistent with the above, a 2-D array is formed. The anion is situated about a 2-fold axis and forms two $\text{Ag}\cdots\text{F}$ contacts less than 3.0 Å, that is, $\text{Ag}\cdots\text{F}1 = 2.689(2)$ Å; the next closest $\text{Ag}\cdots\text{F}$ contact is $\text{Ag}\cdots\text{F}2^1 = 3.112(2)$ Å; $i: 2-x, 1-y, -z$. The $\text{Ag}\cdots\text{F}1$ interactions link the dimers into rows aligned with the c -axis. Two of the F atoms participate in $\text{N}-\text{H}\cdots\text{F}$ interactions leading to a 2-D array as shown in Figure 7D, and these are complemented by weaker $\text{C}-\text{H}\cdots\text{F}$ contacts (not shown).³⁸ The organic residues of adjacent rows overlap somewhat allowing for the formation of $\pi\cdots\pi$ interactions between the five-membered N2, N3, C6–C8, and aromatic C7–C12 rings.³⁸ The topology of the resulting layer, which accommodates the dianions within, is undulating, Figure 7E, and

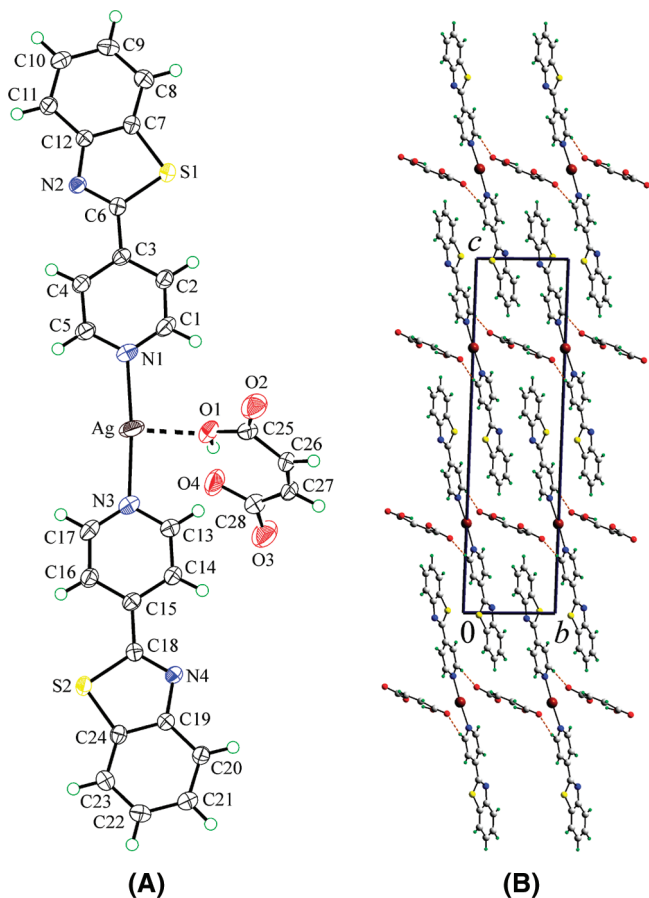


Figure 5. Views of the structure of $[\text{Ag}(\text{L}^2)_2(\text{HO}_2\text{CC}(\text{H})=\text{C}(\text{H})\text{-CO}_2)]_n$ (**2b**): (A) Crystallographic asymmetric unit showing atomic numbering scheme; intermolecular $\text{Ag}\cdots\text{O}$ interaction is shown as a dashed line. (B) Crystal packing viewed down the a -axis; $\text{C}-\text{H}\cdots\text{O}$ interactions are shown as orange-dashed lines.

the primary connections between layers stacked along the b -axis are of the type $\text{C}-\text{H}\cdots\pi$.³⁸

The structures of **4a** and **4b** are readily derived from the previous series in that the imine group in the ligand has been replaced by a sulfur atom, and thereby, a potent crystal structure-directing source has been removed. Centrosymmetric dimers with extended chair conformations are found in each of $[\text{Ag}(\text{L}^4)(\text{NO}_3)]_2$ (**4a**) and $[\text{Ag}(\text{L}^4)(\text{O}_3\text{SCF}_3)]_2$ (**4b**), Figures 8A and B. Deviations from linear coordination geometries of Ag ion are again apparent and are traced to the influence of $\text{Ag}\cdots\text{O}$, F interactions, with $\text{Ag}-\text{N}2$, $\text{N}1^i = 2.219(3)$ and $2.225(3)$ Å, $\text{N}2-\text{Ag}-\text{N}1^i = 144.0(1)^\circ$ for **4a**, and $2.216(2)$, $2.202(2)$ Å, and $\text{N}2-\text{Ag}-\text{N}1^i = 147.54(7)^\circ$ for **4b**, (i) $1-x, 1-y, 1-z$. The key supramolecular aggregation in the crystal structure of **4a** involves interionic $\text{Ag}\cdots\text{O}$ interactions that lead to a supramolecular oligomer, orientated along the a -axis, comprising dimeric cations interspersed by pairs of nitrate anion, Figure 9. In this pattern, each nitrate binds one Ag atom ($\text{Ag}\cdots\text{O}1 = 2.565(3)$ Å) and simultaneously “chelates” a second Ag atom of a neighboring dimeric unit ($\text{Ag}\cdots\text{O}2^{\text{ii}}$, $\text{O}3^{\text{ii}} = 2.617(4)$, $2.824(4)$ Å, (ii) $-x, 1-y, 1-z$). Adjacent chains interdigitate allowing for the formation of $\text{C}-\text{H}\cdots\text{O}$ contacts between them.³⁹ The packing appears to allow for $\pi\cdots\pi$ interactions but the shortest ring centroid...ring centroid distance is quite long at $3.969(2)$ Å.³⁹ Should the aforementioned $\text{C}-\text{H}\cdots\text{O}$ and $\pi\cdots\pi$ interactions be considered significant, the global

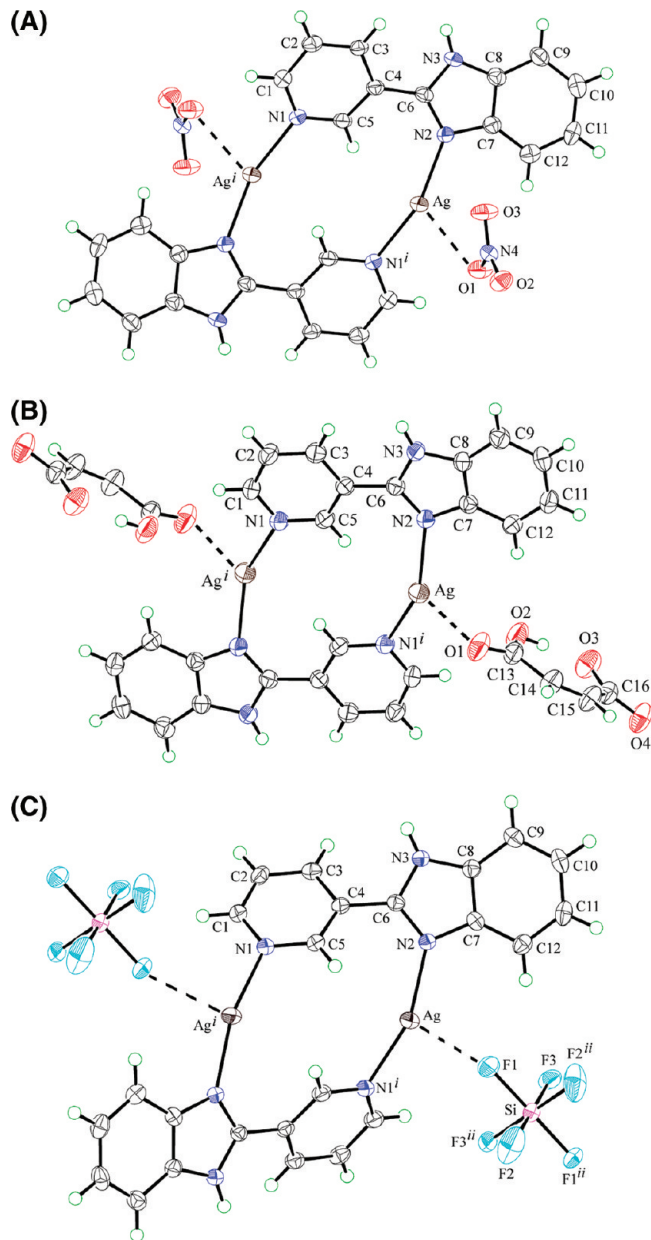


Figure 6. Dimeric aggregates and loosely associated anions showing atomic numbering schemes for (A) $[\text{Ag}(\text{L}^3)(\text{NO}_3)]_2$ (**3a**), (B) $[\text{Ag}(\text{L}^3)(\text{HO}_2\text{CC}(\text{H})=\text{C}(\text{H})\text{CO}_2)]_2$ (**3b**), and (C) $[\text{Ag}(\text{L}^3)(\text{SiF}_6)_{0.5}]_2$ (**3c**). Intermolecular $\text{Ag}\cdots\text{O}$ and $\text{Ag}\cdots\text{F}$ interactions are shown as dashed lines. Symmetry codes: (A) (i) $1-x, 1-y, 1-z$; (B) (i) $-x, -y, 1-z$; (C) (i) $2-x, y, 1/2-z$, (ii) $2-x, y, -1/2-z$.

crystal packing might be described as being comprised of layers. Each of the triflate-O atoms in the isostructural **4b**, forms a contact with the Ag atom but one distance ($\text{Ag}\cdots\text{O}2^i = 3.046(2)$ Å) is significantly longer than the other two, that is, $\text{Ag}\cdots\text{O}1$, $\text{O}3^i = 2.601(2)$ and $2.612(2)$ Å, and must be considered marginal, (i) $-x, 1-y, 1-z$. Nevertheless, the resulting supramolecular chain resembles closely to that seen in the structure of **4a** where the bridging anions linked the dimeric units to form a supramolecular chain. Interdigitation is again facilitated by $\text{C}-\text{H}\cdots\text{O}$ contacts between adjacent chains in **4b** and there is evidence for $\pi\cdots\pi$ interactions.³⁹

Influence of Counter Ions. The anions used here have profound influence in controlling the molecular architectures through supramolecular contacts, namely, $\text{Ag}\cdots\text{O}$

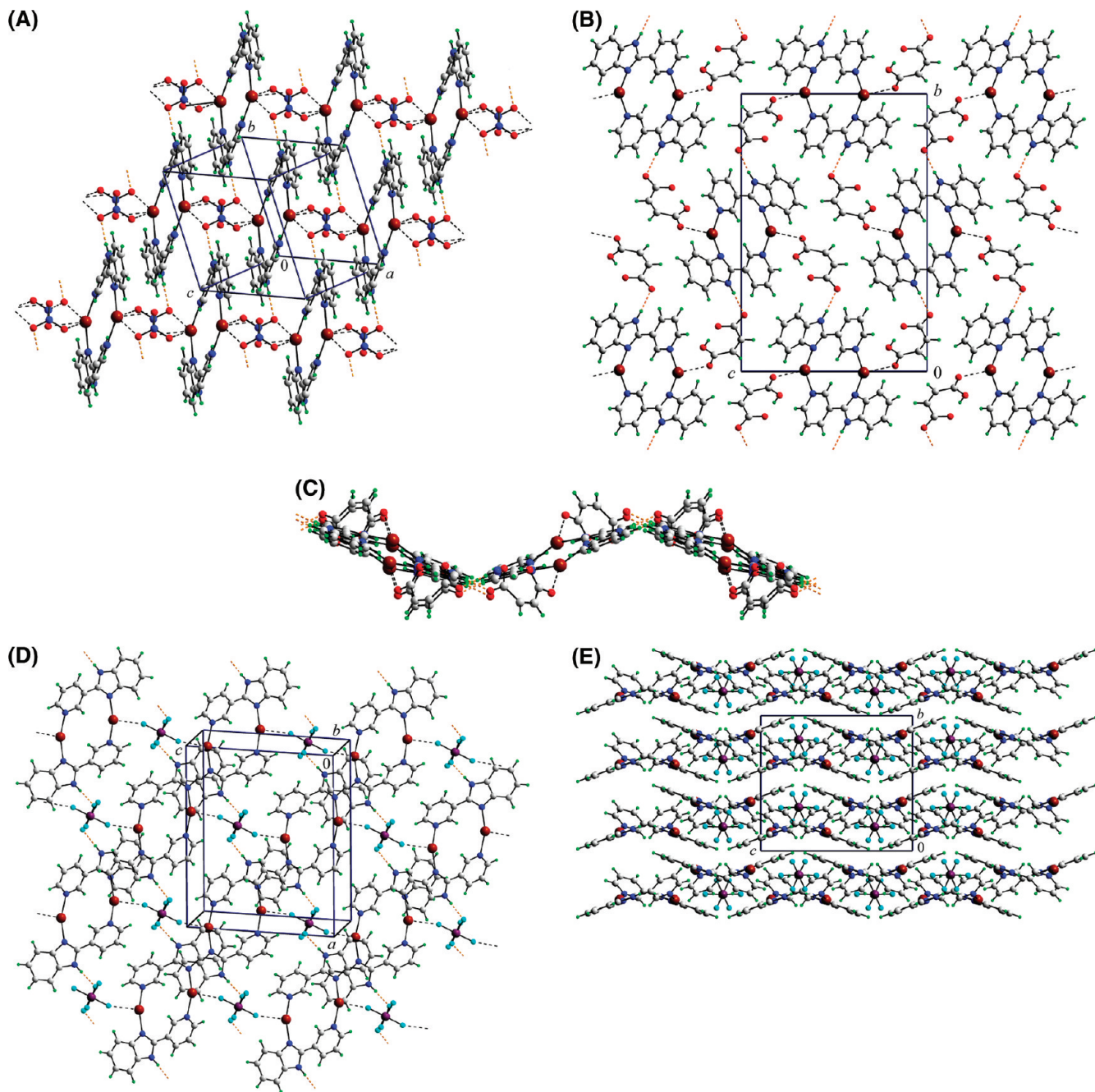


Figure 7. (A) Crystal packing in $[\text{Ag}(\text{L}^3(\text{NO}_3))_2]$ (**3a**) highlighting the 2-D array, (B) unit cell contents for $[\text{Ag}(\text{L}^3(\text{HO}_2\text{CC}(\text{H})=\text{C}(\text{H})\text{CO}_2))_2]$ (**3b**) viewed down the a -axis, (C) undulating topology of the 2-D array in (**3b**) viewed down $(-1\ 0\ 3)$, (D) crystal packing in $[\text{Ag}(\text{L}^3(\text{SiF}_6)_{0.5})_2]$ (**3c**) highlighting the 2-D array, and (E) stacking of undulating layers in (**3c**). Intermolecular $\text{Ag}\cdots\text{O}$ and $\text{Ag}\cdots\text{F}$ interactions are shown as dashed lines, and $\text{N}-\text{H}\cdots\text{O}$, F hydrogen bonding is shown as orange-dashed lines.

and $\text{Ag}\cdots\text{F}$ secondary bonding (**1b**, **2b**, **3a–3c**, **4a**, **4b**) and $\text{O}-\text{H}\cdots\text{O}$ (**1a**, **2a**, **2b**), $\text{N}-\text{H}\cdots\text{O}$, F (**1b**, **2b**, **3a–3c**), and $\text{C}-\text{H}\cdots\text{O}$, F (**2b**, **3a–3c**) hydrogen bonding. As the ligands L^2 and L^4 have no NH hydrogen donor, most of the anions prefer to interact only with the silver(I) ion as in **2a**, **2b**, **4a** and **4b**. By contrast, the presence of the NH group in the ligands L^1 and L^3 facilitates the formation of $\text{N}-\text{H}\cdots\text{O}$, F hydrogen bonds. Thus in **1a**, NO_3^- prefers to bind only the ligand, while in other compounds, namely, **1b** and **3a–3c**, the anions, including NO_3^- , are attached to both the ligands as well as the silver(I) ion. Bridging through the anions in some of the structures has a dominating influence upon the overall crystal packing. Thus, CF_3COO^- bridges strongly in **1b** and

controls the network formation. Also, an undulating topology of the layers in **3c** is favored by the bridging interaction of SiF_6^{2-} anion (Figure 7E). However, similar interactions of the other anions in **3a**, **4a**, and **4b** are too weak to show any significant influence upon the overall supramolecular architectures.

Photophysical Properties. In CH_3OH , the free ligands (L^1-L^4) show two absorption peaks in the regions 311–299 and 255–240 nm attributable to $\pi-\pi^*$ transitions centered at the 2-pyridin-3/4-yl-benzoimidazolyl/benzothiazolyl moieties.

The fluorescence, phosphorescence and excitation spectra of the free ligands have been recorded both in the solid state

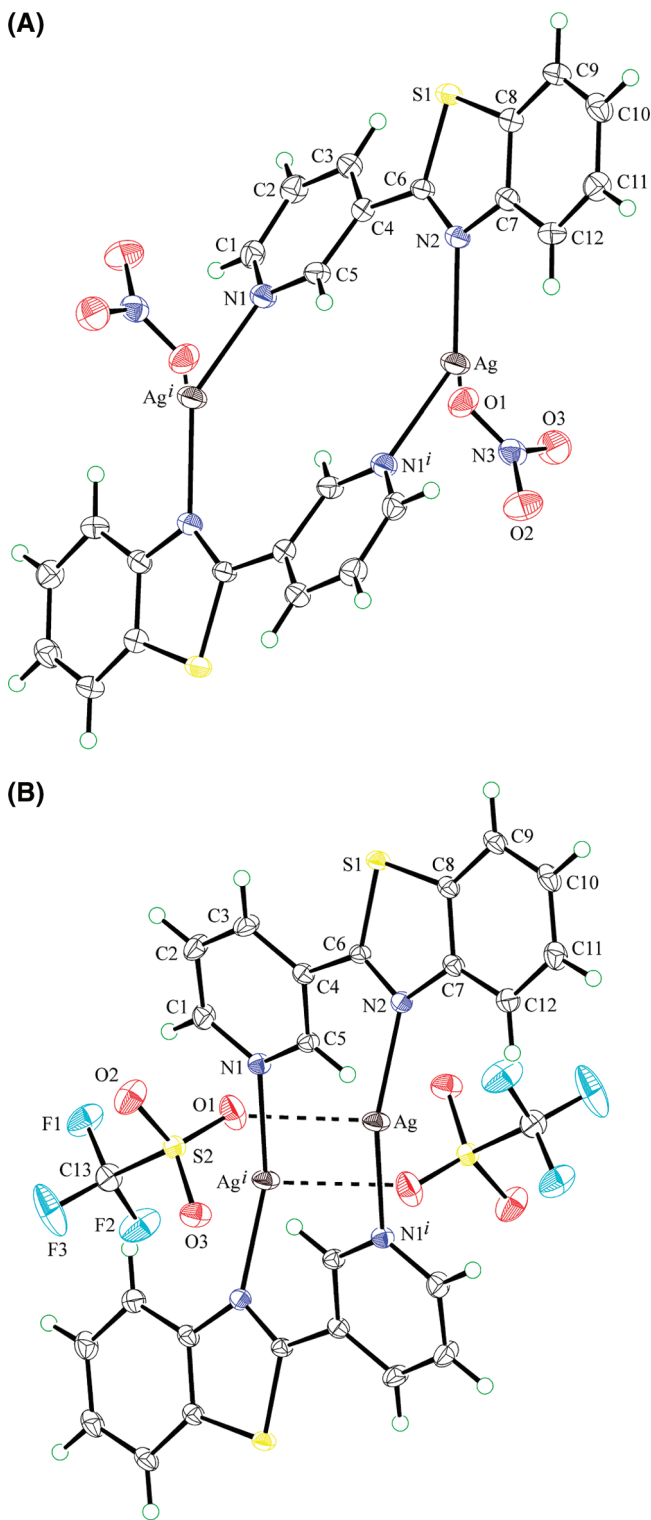


Figure 8. Dimeric aggregates and loosely associated anions showing atomic numbering schemes for (A) $[\text{Ag}(\text{L}^4)(\text{NO}_3)_2]$ (**4a**) and (B) $[\text{Ag}(\text{L}^4)(\text{O}_3\text{SCF}_3)_2]$ (**4b**). Intermolecular $\text{Ag}\cdots\text{O}$ interactions are shown as dashed lines. Symmetry codes: (A) (i) $1-x, 1-y, 1-z$; (B) (i) $-x, -y, -z$.

as well as in solution at 298 and 77 K. The spectra for the complexes are studied only in the solid state at 77 K as these are only sparingly soluble in common organic solvents as well as in water. The results are summarized in Tables 4 and 5. All the complexes including the ligands show both fluorescence and phosphorescence in the solid state at this

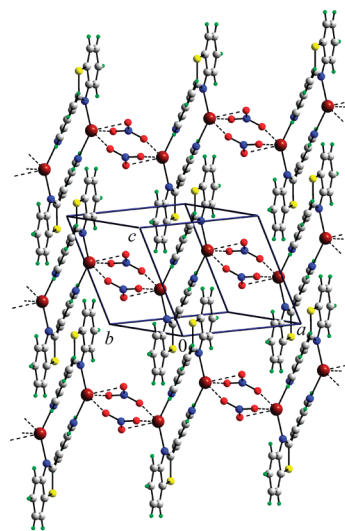


Figure 9. Crystal packing diagram for $[\text{Ag}(\text{L}^4)(\text{NO}_3)_2]$ (**4a**). Intermolecular $\text{Ag}\cdots\text{O}$ interactions are shown as dashed lines.

Table 4. Emission Spectral and Phosphorescence Lifetime Data for the Complexes **1a**, **1b**, **2a**, **2b**, **3a–3c**, **4a**, and **4b** and Free Ligands L^1 – L^4 at 77 K

compound	fluorescence λ/nm	position of the phosphorescence (0, 0) band (nm)	phosphorescence lifetime (sec)	medium
L^1	380	451	2.4	CH_3OH
	407	485	2.4	solid
1a	394	495	0.6	solid
1b	394	517	0.6	solid
L^2	396	487	2.3	CH_3OH
	418	510	2.3	solid
2a	465	554	0.7	solid
2b	431	566	0.6	solid
L^3	365	446	3.3	CH_3OH
	403	522	3.3	solid
3a	377	467	0.6	solid
3b	373	480	0.5	solid
3c	352	464	0.7	solid
L^4	380	486	3.0	CH_3OH
	375	502	3.0	solid
4a	404	513	0.5	solid
4b	428	507	0.8	solid

Table 5. Fluorescence Lifetimes^a for L^2 and the Complexes **2a** and **2b**

	L^2 glass ^b	L^{2c}	2a ^c	2b ^c
τ_1	0.75 (85.5%)	0.74 (86.5%)	0.4 (97%)	0.5 (100%)
τ_2	4.2 (14.5%)	3.9 (13.5%)	2.7 (3%)	

^a in ns. ^b In methanol glass at 77 K. ^c In solid at 77 K.

temperature. The free ligands in CH_3OH solution also display both fluorescence and phosphorescence. A dramatic red-shift was observed for emission of the complexes and the ligands in the solid state with respect to the ligand in solution, which is caused by intermolecular interactions in the solid state that effectively decrease the energy gaps between the concerned energy states. The fluorescence maxima of **1a**, **1b**, **3a**, **3b**, and **3c** are less intense and blue-shifted with respect to the free ligands L^1 and L^3 in the solid state, while the complexes **2a**, **2b** and **4a**, **4b** exhibit fluorescence with band maxima at 465, 431, 404, and 428 nm, respectively; these values are red-shifted from the fluorescence of the corresponding free ligands L^2 and L^4 (418 and 375 nm, respectively). The excitation spectra and the corresponding life

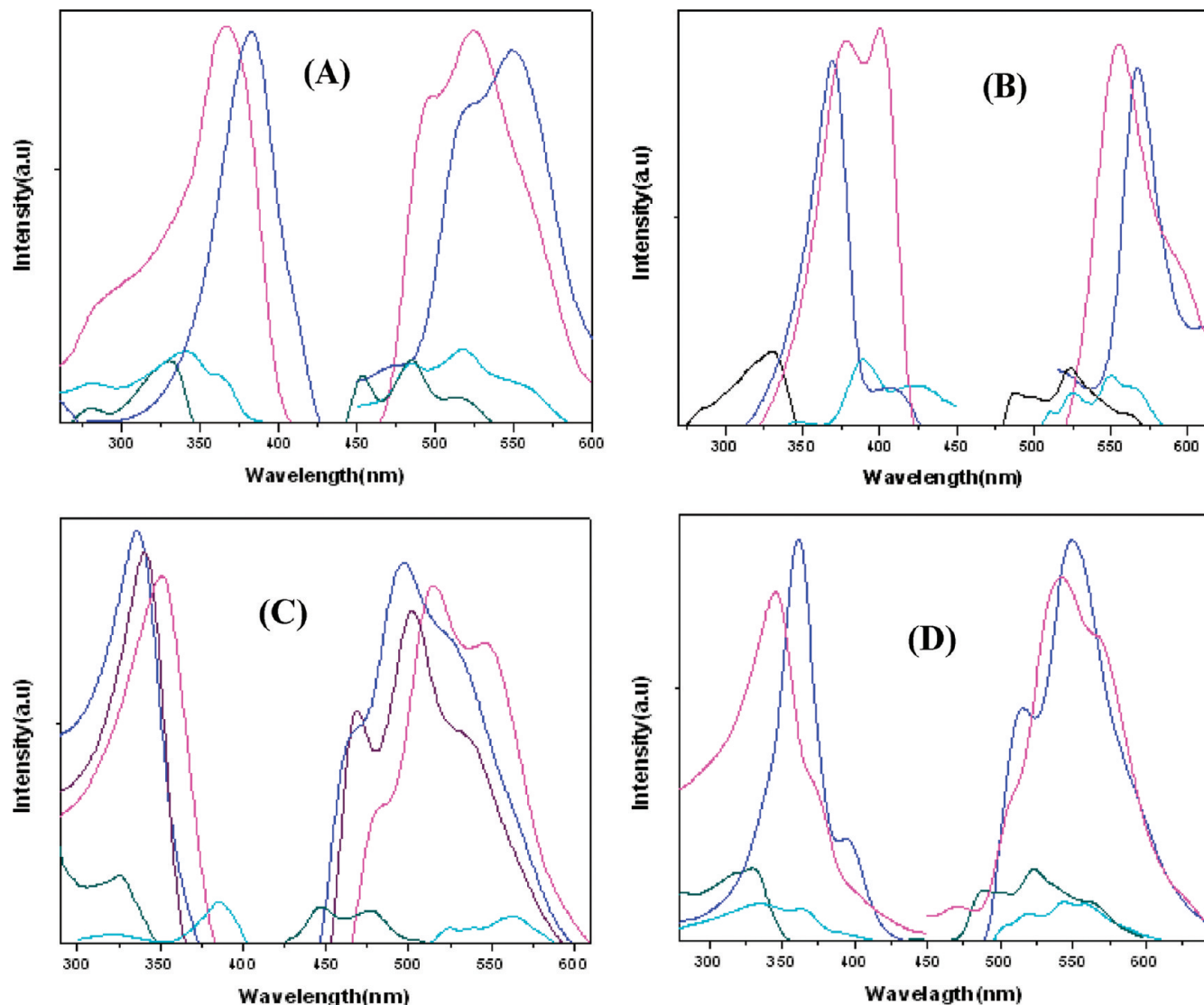


Figure 10. Phosphorescence excitation and emission spectra of the free ligands and their silver complexes with different counteranions at 77 K: (A) L^1 in solid (cyan), L^1 in methanol solution (gray), **1a** (magenta), **1b** (blue), (B) L^2 in solid (cyan), L^2 in methanol solution (gray), **2a** (magenta), **2b** (blue), (C) L^3 in solid (cyan), L^3 in methanol solution (gray), **3a** (red), **3b** (magenta), **3c** (blue), (D) L^4 in solid (cyan), L^4 in methanol solution (gray), **4a** (blue), **4b** (magenta); excitation band-pass = 10 nm, emission band-pass = 2.5 nm.

times in nanosecond range suggest that π - π^* intraligand transitions are responsible for the fluorescence. A substantial amount of red-shift for **2a**, **2b** and **4a**, **4b** is indicative of a marginal MLCT contribution over and above the ligand-localized π - π^* transition. Weak intermolecular $\text{Ag}\cdots\text{Ag}$ interactions in **2a** are probably responsible for the more pronounced red shift in the emission energy of this compound.

The phosphorescence spectra for the ligands and their complexes in the solid state together with those of the free ligands in solution at 77 K are shown in Figure 10. The observed enhancements in the phosphorescence of the complexes result from substantial spin-orbit coupling provided by the heavy atom Ag.⁴⁰ To access the extent of this heavy atom effect, we analyzed the phosphorescence lifetimes for the free ligands and the complexes. Interestingly, the complexes have triplet lifetimes in the range 0.5–0.8 s, much shorter than the lifetimes for the free ligands (2.3–3.3 s) as reported recently by Gabbai et al.^{40a,40c} The crystal structure analyses of the silver complexes reveal that there are short

$\text{Ag}-\text{C}_{\text{aromatic}}$ contacts in the range 2.9–4.1 Å in **1a**, **2a**, **3a**, **3b**, and **3c** (Ag -ring centroid distances for these compounds are 3.19, 3.54 and 3.70, 3.97, 3.43, 3.77 Å, respectively), suggesting the presence of secondary $\text{Ag}\cdots\pi$ interactions. While the Ag(I) complex of L^1 with NO_3^- anion (**1a**) has a strong $\text{Ag}\cdots\pi$ interaction (Figure 11), there is no appreciable interaction present in **1b**, with CF_3COO^- as counteranion. The same phosphorescence lifetime (0.6 s) for these two complexes suggest that the internal heavy atom perturbation due to the presence of the Ag atom in close proximity (bonding distance) to the chromophore makes the internal heavy atom effect overwhelm the external heavy atom effect (secondary metal $\cdots\pi$ interaction) and the triplet lifetimes remain almost unperturbed due to the external effect. Moreover, the lifetime reduction with respect to the free ligands is more drastic for complexes with 2-pyridin-3-yl-benzimidazole/benzothiazole ligands (**3a–3c**, **4a**, **4b**) relative to 2-pyridin-4-yl-benzimidazole/benzothiazole ligands (**1a**, **1b**, **2a**, **2b**). The spin orbit coupling inducing the heavy atom effect depends not only on the distance of the heavy atom perturber

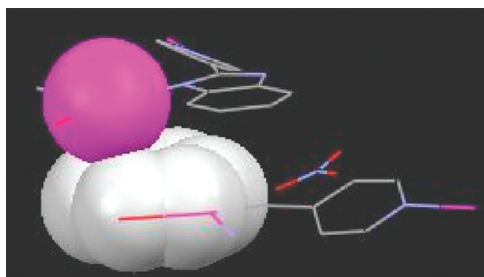


Figure 11. Metal- π interaction in **1a**; Ag- π centroid distance is 3.19 Å.

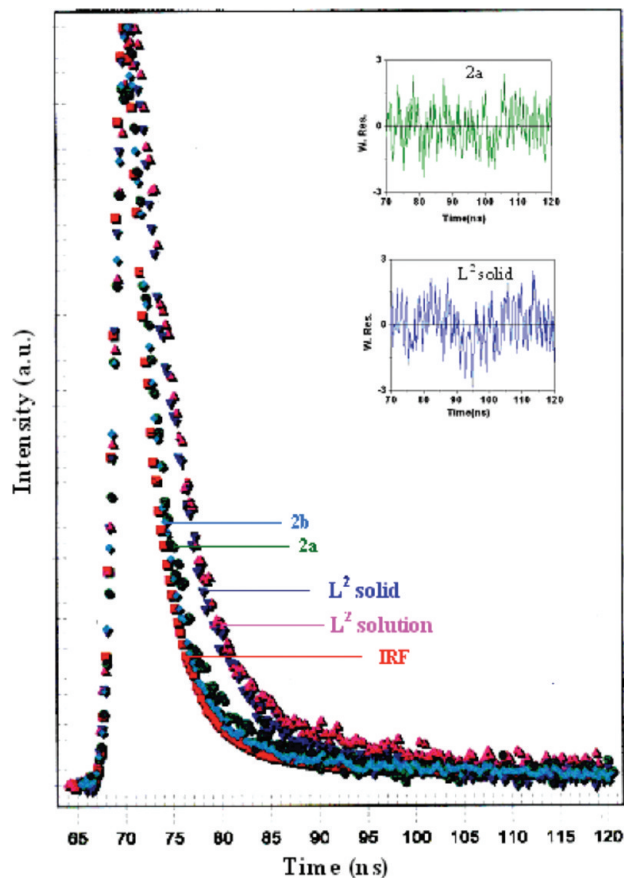


Figure 12. Fluorescence decay of L^2 in solid state (blue), in methanol solution (magenta), **2a** (green), **2b** (cyan) at 77 K, $\lambda_{exc} = 330$ nm; excitation and emission band passes are 10 nm each. Inset: χ^2 of solid L^2 (blue) and **2a** (green).

from the π -system but also on the orientation of the perturber with respect to the π -plane of the ligand.⁴¹ Thus, in the cases of **3a–3c** and **4a, 4b** it appears that the orientations of the Ag^+ ion with respect to the π -plane of the ligands are favorable for enhanced spin orbit coupling.

Measured fluorescence lifetimes for the complexes are also much shorter than the free ligands at 77 K. Figure 12 represents the fluorescence decay of the free ligand L^2 in solution and in solid together with its Ag-complexes **2a** and **2b** in the solid state at 77 K. The χ^2 values are found to be close to 1 in all cases (two are shown in the inset of Figure 12). The decays for L^2 in methanol glass and in the solid state at 77 K are found to fit two exponentials. The shorter lifetime (0.75 ns) contributes 86% while the contribution of the longer component (~ 4 ns) is 14% (Table 5). The lifetimes

of the complexes reduce to 0.4 ns with 97% contribution in the case of **2a** whereas the complex **2b** shows a single component of 0.5 ns. The shortening of fluorescence lifetimes further supports the presence of heavy atom effect which increases the nonradiative rate $S_1 \rightarrow T_1$ in the complexes.

Concluding Remarks

A series of silver(I) complexes with rigid multiring heterocyclic ligands (L^1-L^4) have been synthesized by the process of self-assembly. Both anions and the ligand donor sets (NH vs S) have a profound influence on the resulting solid state structures in which the Ag atoms have either linear, T-shaped or tetrahedral geometries. Supramolecular contacts such as hydrogen bonding, $\pi \cdots \pi$ stacking and C-H $\cdots\pi$ interactions, all consolidate the crystal packing. In the solid state these compounds are all photoactive at 77 K exhibiting phosphorescent emissions which are likely to originate from the intraligand $\pi-\pi^*$ transitions with enhanced intensity due to coordination to the silver(I) ion. Both counteranions as well as ligand donor sets (S vs NH) have marked influence on the emission properties of these compounds.

Acknowledgment. This work was supported by the Council of Scientific and Industrial Research (CSIR), New Delhi. N. K., A.A., and S.M.T.A thank the CSIR for the award of Research Fellowships. S.G. also thanks CSIR and DST for financial support.

Supporting Information Available: X-ray crystallographic files in CIF format for the complexes **1a, 1b, 2a, 2b, 3a–3c, 4a, and 4b**. This material is available free of charge via the Internet at <http://pubs.acs.org>.

References

- (1) (a) Yaghi, O. M.; Li, H. L.; Davis, C.; Richardson, D.; Groy, T. L. *Acc. Chem. Res.* **1998**, *31*, 474. (b) Batten, R. S.; Robson, R. *Angew. Chem., Int. Ed.* **1998**, *37*, 1460. (c) Fujita, M. *Chem. Soc. Rev.* **1998**, *27*, 417. (d) Braunstein, P.; Oro, L. A.; Raithby, P. R. *Metal Clusters in Chemistry*; Wiley-VCH: New York, 1999. (e) Hidai, M.; Kuwata, S.; Mizobe, Y. *Acc. Chem. Res.* **2000**, *33*, 46. (f) Eddaoudi, M.; Kim, J.; Rosi, N.; Vodak, D.; Wachter, J.; O'Keeffe, M.; Yaghi, O. M. *Science* **2002**, *295*, 469. (g) Kitagawa, S.; Kitaura, R.; Noro, S.-i. *Angew. Chem.* **2004**, *116*, 2388. (h) Goicoechea, J. M.; Sevov, S. C. *Angew. Chem., Int. Ed.* **2005**, *44*, 4026. (i) Kitagawa, S.; Noro, S.-i.; Nakamura, T. *Chem. Commun.* **2006**, 701. (j) Rowsell, J. L. C.; Yaghi, O. M. *J. Am. Chem. Soc.* **2006**, *128*, 1304. (k) Tranchemontagne, D. J.; Mendoza-Cortes, J. L.; O'Keeffe, M.; Yaghi, O. M. *Chem. Soc. Rev.* **2009**, *38*, 1257.
- (2) (a) Lehn, J. M. *Supramolecular Chemistry: Concepts and Perspectives*; VCH: Weinheim, Germany, 1995. (b) Adams, R. D.; Cotton, F. A. *Catalysis by Di- and Polynuclear Metal Cluster Complexes*; Wiley-VCH: New York, 1998. (c) Blake, A. J.; Champness, N. R.; Hubberstey, P.; Li, W.-S.; Schröder, M.; Withersby, M. A. *Coord. Chem. Rev.* **1999**, *183*, 117. (d) Swiegers, G. F.; Malefetse, T. J. *Chem. Rev.* **2000**, *100*, 3483. (e) Eddaoudi, M.; Moler, D. B.; Li, H.; Chen, B.; Reineke, T. M.; O'Keeffe, M.; Yaghi, O. M. *Acc. Chem. Res.* **2001**, *34*, 319. (f) Moulton, B.; Zaworotko, M. J. *Chem. Rev.* **2001**, *101*, 1629. (g) Batten, S. R.; Murray, K. S. *Coord. Chem. Rev.* **2003**, *246*, 103. (h) Yaghi, O. M.; O'Keeffe, M.; Ockwig, N. W.; Chae, H. K.; Eddaoudi, M.; Kim, J. *Nature* **2003**, *423*, 705. (i) Anthony, S. P.; Radhakrishnan, T. P. *Cryst. Growth Des.* **2004**, *4*, 1223. (j) Ockwig, N. W.; Delgado-Friedrichs, O.; O'Keeffe, M.; Yaghi, O. M. *Acc. Chem. Res.* **2005**, *38*, 176. (k) Han, H.; Song, Y.; Hou, H.; Fan, Y.; Zhu, Y. *Dalton Trans.* **2006**, 1972. (l) Lin, P.; Clegg, W.; Harrington, R. W.; Henderson, R. A.; Fletcher, A. J.; Bell, J.; Thomas, K. M. *Inorg. Chem.* **2006**, *45*, 4284. (m) Guo, X.; Zhu, G.; Li, Z.; Chen, Y.; Li, X.; Qiu, S. *Inorg. Chem.* **2006**, *45*, 4065. (n) Férey, G. *Chem. Soc. Rev.* **2008**, *37*, 191. (o) Ma, L.; Abney, C.; Lin, W. *Chem. Soc. Rev.* **2009**, *38*, 1248. (p) Trzaska, A. U.; Trukhan, N.; Muller, U. *Chem. Soc. Rev.* **2009**, *38*, 1284.

- (q) Murray, L. J.; Dinca, M.; Long, J. R. *Chem. Soc. Rev.* **2009**, *38*, 1294. (r) Lee, J.; Farha, O. K.; Roberts, J.; Scheidt, K. A.; Nguyen, S. T.; Hupp, J. T. *Chem. Soc. Rev.* **2009**, *38*, 1450. (s) Li, J.-R.; Kuppler, R. J.; Zhou, H.-C. *Chem. Soc. Rev.* **2009**, *38*, 1477. (t) Dong, Y.-B.; Jiang, Y.-Y.; Li, J.; Ma, J.-P.; Liu, F.-L.; Tang, B.; Huang, R.-Q.; Batten, S. R. *J. Am. Chem. Soc.* **2007**, *129*, 4520. (u) Zang, S.-Q.; Zhao, L.; Mak, T. C. W. *Organometallics* **2008**, *27*, 2396.
- (3) (a) Rowsell, J. L. C.; Yaghi, O. M. *Angew. Chem., Int. Ed.* **2005**, *44*, 4670. (b) Rowsell, J. L. C.; Eckert, J.; Yaghi, O. M. *J. Am. Chem. Soc.* **2005**, *127*, 14904.
- (4) (a) Zheng, N.; Yassar, A.; Antoun, T.; Yaghi, O. M. *J. Am. Chem. Soc.* **2005**, *127*, 12752. (b) Rowsell, J. L. C.; Spencer, E. C.; Eckert, J.; Howard, J. A. K.; Yaghi, O. M. *Science* **2005**, *309*, 1350.
- (5) (a) Wu, Q.; Esteghamatian, M.; Hu, N.-X.; Popovic, Z. D.; Enright, G.; Tao, Y.; D'lorio, M.; Wang, S. *Chem. Mater.* **2000**, *12*, 79. (b) Kunugi, Y.; Mann, K. R.; Miller, L.; Exstrom, C. L. *J. Am. Chem. Soc.* **1998**, *120*, 589. (c) Vickery, J. C.; Olmstead, M. M.; Fung, E. Y.; Bulch, A. L. *Angew. Chem., Int. Ed.* **1997**, *36*, 1179.
- (6) (a) De Santis, G.; Fabbri, L.; Licchelli, M.; Poggi, A.; Taglietti, A. *Angew. Chem., Int. Ed.* **1996**, *35*, 202. (b) Bulovic, V.; Gu, G.; Burrows, P. E.; Forest, S. R. *Nature* **1996**, *380*, 29. (c) Shirota, Y.; Kuwabara, Y.; Inada, H.; Wakimoto, T.; Nakada, H.; Yonemoto, Y.; Kawami, S.; Imai, K. *Appl. Phys. Lett.* **1994**, *65*, 807.
- (7) (a) Chae, H. K.; Siberio, D. Y.; Kim, J.; Go, Y.; Eddaoudi, M.; Matzger, A. J.; O'Keeffe, M.; Yaghi, O. M. *Nature* **2004**, *427*, 523. (b) Xiong, R.-G.; Xue, X.; Zhao, H.; You, X.-Z.; Abrahams, B. F.; Xue, Z. *Angew. Chem., Int. Ed.* **2002**, *41*, 3800.
- (8) (a) Seo, J. S.; Whang, D.; Lee, H.; Jun, S. I.; Oh, J.; Jeon, Y. J.; Kim, K. *Nature* **2000**, *404*, 982. (b) Kahn, O.; Martinez, C. *Science* **1998**, *279*, 44. (c) Tong, M.-L.; Chen, X.-M.; Ye, B.-H.; Ji, L.-N. *Angew. Chem., Int. Ed.* **1999**, *38*, 2237.
- (9) (a) Janiak, C. *J. Chem. Soc., Dalton Trans.* **2000**, 3883. (b) Robin, A. Y.; Fromm, K. M. *Coord. Chem. Rev.* **2006**, *250*, 2127. (c) Kaes, C.; Hosseini, M. W.; Rickard, C. E. F.; Skelton, B. W.; White, A. H. *Angew. Chem., Int. Ed.* **1998**, *37*, 920. (d) Mislin, G.; Graf, E.; Hosseini, M. W.; Cian, A. D.; Kyritsakas, N.; Fischer, J. *Chem. Commun.* **1998**, 2545. (e) Dorn, T.; Fromm, K. M.; Janiak, C. *Aust. J. Chem.* **2006**, *59*, 22. (f) Khlobystov, A. N.; Blake, A. J.; Champness, N. R.; Lemenovskii, D. A.; Majouga, A. G.; Zyk, N. V.; Schröder, M. *Coord. Chem. Rev.* **2001**, *222*, 155. (g) Santillan, G. A.; Carrano, C. J. *Cryst. Growth Des.* **2009**, *9*, 1590. (h) Matsumoto, K.; Harada, Y.; Yamada, N.; Kurata, H.; Kawase, T.; Oda, M. *Cryst. Growth Des.* **2006**, *6*, 1083. (i) Oh, M.; Stern, C. L.; Mirkin, C. A. *Inorg. Chem.* **2005**, *44*, 2647. (j) Hollis, C. A.; Hanton, L. R.; Morris, J. C.; Sumbly, C. J. *Cryst. Growth Des.* **2009**, *9*, 2911. (k) Silva, R. M.; Smith, M. D.; Gardinier, J. R. *Inorg. Chem.* **2006**, *45*, 2132. (l) Pigge, F. C.; Burgard, M. D.; Rath, N. P. *Cryst. Growth Des.* **2003**, *3*, 331. (m) Brandys, M. -C.; Puddephatt, R. J. *J. Am. Chem. Soc.* **2002**, *124*, 3946. (n) Habata, Y.; Noto, K.; Osaka, F. *Inorg. Chem.* **2007**, *46*, 6529.
- (10) (a) Baldo, M. A.; O'Brien, D. F.; You, Y.; Shoustikov, A.; Sibley, S.; Thompson, M. E.; Forrest, S. R. *Nature* **1998**, *395*, 151. (b) Baldo, M. A.; Lamansky, S.; Burrows, P. E.; Thompson, M. E.; Forrest, S. R. *Appl. Phys. Lett.* **1999**, *75*, 4. (c) Baldo, M. A.; O'Brien, D. F.; Thompson, M. E.; Forrest, S. R. *Phys. Rev. B* **1999**, *60*, 14422. (d) Adachi, C.; Baldo, M. A.; Forrest, S. R.; Thompson, M. E. *Appl. Phys. Lett.* **2000**, *77*, 904. (e) Lamansky, S.; Djurovich, P.; Murphy, D.; Abdel-Razzaq, F.; Lee, H.; Adachi, C.; Burrows, P. E.; Forrest, S. R.; Thompson, M. E. *J. Am. Chem. Soc.* **2001**, *123*, 4304. (f) Adamovich, V.; Brooks, J.; Tamayo, A.; Alexander, A. M.; Djurovich, P. I.; D'Andrade, B. W.; Adachi, C.; Forrest, S. R.; Thompson, M. E. *New J. Chem.* **2002**, *26*, 1171. (g) Sun, Y.; Giebink, N. C.; Kanno, H.; Ma, B.; Thompson, M. E.; Forrest, S. R. *Nature* **2006**, *440*, 908.
- (11) (a) Ikai, M.; Tokito, S.; Sakamoto, Y.; Suzuki, T.; Taga, Y. *Appl. Phys. Lett.* **2001**, *79*, 156. (b) Chen, F. C.; Yang, Y.; Thompson, M. E.; Kido, J. *Appl. Phys. Lett.* **2002**, *80*, 2308. (c) Baldo, M. A.; Thompson, M. E.; Forrest, S. R. *Nature* **2000**, *403*, 750.
- (12) Slinker, J.; Bernards, D.; Houston, P. L.; Abruña, H. D.; Bernhard, S.; Malliaras, G. G. *Chem. Commun.* **2003**, 2392.
- (13) Rudmann, H.; Shimida, S.; Rubner, M. F. *J. Am. Chem. Soc.* **2002**, *124*, 4918.
- (14) Bernhard, S.; Barron, J. A.; Houston, P. L.; Abruna, H. D.; Ruglovsky, J. L.; Gao, X.; Malliaras, G. G. *J. Am. Chem. Soc.* **2002**, *124*, 13624.
- (15) Wegh, R. T.; Meijer, E. J.; Plummer, E. A.; De Cola, L.; Brunner, K.; van Dijken, A.; Hofstra, J. W. *Proc. SPIE* **2004**, *5519*, 48.
- (16) Slinker, J. D.; Gorodetsky, A. A.; Lowry, M. S.; Wang, J.; Parker, S.; Rohl, R.; Bernhard, S.; Malliaras, G. G. *J. Am. Chem. Soc.* **2004**, *126*, 2763.
- (17) Pass, H. I. *J. Natl. Cancer Inst.* **1993**, *85*, 443.
- (18) Handy, E. S.; Pal, A. J.; Rubner, M. F. *J. Am. Chem. Soc.* **1999**, *121*, 3525.
- (19) (a) Know, C.-C.; Yu, S.-C.; Sham, I. H. T.; Che, C.-M. *Chem. Commun.* **2004**, 2758. (b) Gao, F. G.; Bard, A. J. *J. Am. Chem. Soc.* **2000**, *122*, 7426.
- (20) Kacelrud, L. *Prog. Polym. Sci.* **2003**, *28*, 875.
- (21) Mitschke, U.; Bauerle, P. *J. Mater. Chem.* **2000**, *10*, 1471.
- (22) Kraft, A.; Grimsdale, A. C.; Holmes, A. B. *Angew. Chem., Int. Ed.* **1998**, *37*, 402.
- (23) Yu, S. C.; Kwok, C. C.; Chan, W. K.; Che, C.-M. *Adv. Mater.* **2003**, *15*, 1643.
- (24) For example, see: (a) O'Kane, S. A.; Clerac, R.; Zhao, H. H.; Xiang, O. Y.; Galan-Mascaros, J. R.; Heintz, R.; Dunbar, K. R. *J. Solid State Chem.* **2000**, *152*, 159. (b) Carlucci, L.; Ciani, G.; Proserpio, D. M. *CrystEngComm* **2003**, *5*, 269. (c) Burchell, T. J.; Puddephatt, R. J. *Inorg. Chem.* **2006**, *45*, 650. (d) Feazell, R. P.; Carson, C. E.; Klausmeyer, K. K. *Inorg. Chem.* **2006**, *45*, 2635. (e) Xie, L. X.; Wei, M. L.; Duan, C. Y.; Sun, Q. Z.; Meng, Q. *J. Inorg. Chim. Acta* **2007**, *360*, 2541. (f) Bellusci, A.; Crispini, A.; Pucci, D.; Szerb, E. I.; Ghedini, M. *Cryst. Growth Des.* **2008**, *8*, 3114.
- (25) (a) Papaefstathiou, G. S.; MacGillivray, L. R. *Coord. Chem. Rev.* **2003**, *246*, 169. (b) Zheng, S. L.; Tong, M. L.; Chen, X. M. *Coord. Chem. Rev.* **2003**, *246*, 185. (c) Cunha-Silva, L.; Ahmad, R.; Hardie, M. J. *Aust. J. Chem.* **2006**, *59*, 40. (d) Steel, P. J.; Fitchett, C. M. *Coord. Chem. Rev.* **2008**, *252*, 990.
- (26) (a) Wang, M.-S.; Guo, S.-P.; Li, Y.; Cai, L.-Z.; Zou, J.-P.; Xu, G.; Zhou, W.-W.; Zheng, F.-K.; Guo, G.-C. *J. Am. Chem. Soc.* **2009**, *131*, 13572. (b) Bellusci, A.; Ghedini, M.; Giorgini, L.; Gozzo, F.; Szerb, E. I.; Crispini, A.; Pucci, D. *Dalton Trans.* **2009**, 7381. (c) Yuan, G.; Zhu, C.; Liu, Y.; Xuan, W.; Cui, Y. *J. Am. Chem. Soc.* **2009**, *131*, 10452. (d) Deng, Z.-P.; Zhu, Z.-B.; Gao, S.; Huo, L.-H.; Zhao, H.; Ng, S. W. *Dalton Trans.* **2009**, 6552. (e) Santillan, G. A.; Carrano, C. J. *Dalton Trans.* **2009**, 6599. (f) Liddle, B. J.; Hall, D.; Lindeman, S. V.; Smith, M. D.; Gardinier, J. R. *Inorg. Chem.* **2009**, *48*, 8404.
- (27) Perrin, D. D.; Armarego, W. L. F.; Perrin, D. R. *Purification of Laboratory Chemicals*, 2nd ed.; Pergamon: Oxford, England, 1980.
- (28) Robinson, W. R. *J. Chem. Educ.* **1985**, *62*, 1001.
- (29) Chatterjee, P. B.; Mandal, D.; Audhya, A.; Choi, K.-Y.; Endo, A.; Chaudhury, M. *Inorg. Chem.* **2008**, *47*, 3709.
- (30) *FELIX 32, Operation Manual*, Version 1.1, Photon Technology International, Inc.: NJ, 2003.
- (31) (a) *SAINTE*, version 5.6. Bruker AXS Inc.: Madison, WI, **2000**; (b) Sheldrick, G. M. *SADABS*. University of Göttingen: Göttingen, Germany, 2000; Blessing, R. *Acta Crystallogr.* **1995**, *A51*, 33. (c) Beurskens, P. T.; Admiraal, G.; Beurskens, G.; Bosman, W. P.; Garcia-Granda, S.; Smits, J. M. M.; Smykalla, C. *The DIRDIF Program System*; Technical Report of the Crystallography Laboratory; University of Nijmegen, Nijmegen, The Netherlands, 1992. (d) Sheldrick, G. M. *Acta Crystallogr.* **2008**, *64*, 112. (e) Johnson, C. K. *ORTEP-II*; Report ORNL-5138; Oak Ridge National Laboratory: Oak Ridge, TN, 1976. (f) *DIAMOND, Visual Crystal Structure Information System*, version 2.1e; Crystal Impact: Bonn, Germany 2002. (g) *teXsan: Structure Analysis Software*; Molecular Structure Corp.: The Woodlands, TX, 1997. (h) Spek, A. L. *J. Appl. Crystallogr.* **2003**, *36*, 7.
- (32) (a) Wattenberg, L. W.; Page, M. A.; Leong, J. L. *Cancer Res.* **1968**, *28*, 2539. (b) Porcari, A. R.; Devivar, R. V.; Kucera, L. S.; Drach, J. C.; Townsend, L. B. *J. Med. Chem.* **1998**, *41*, 1251. (c) Roth, M.; Morningstar, M. L.; Boyer, P. L.; Hughes, S. H.; Bukheit, R. W.; Michejda, C. J. *J. Med. Chem.* **1997**, *40*, 4199. (d) Migawa, M. T.; Giradet, J. L.; Walker, J. A.; Koszalka, G. W.; Chamberlain, S. D.; Drach, J. C.; Townsend, L. B. *J. Med. Chem.* **1998**, *41*, 1242.
- (33) Tebbe, M. J.; Spitzer, W. A.; Victor, F.; Miller, S. C.; Lee, C. C.; Sattelberg, T. R.; McKinney, E.; Tang, C. J. *J. Med. Chem.* **1997**, *40*, 3937.
- (34) Nancashire, R. J. In *Comprehensive Coordination Chemistry*; Wilkinson, G.; Gillard, R. D.; McCleverty, J. A., Eds.; Pergamon: Oxford, U.K., 1987; Vol. 5, Chapter 54.
- (35) Nakamoto, K. *Infrared and Raman Spectra of Inorganic and Coordination Compounds* 5th ed.; Wiley-Interscience: New York, 1997.
- (36) Intermolecular interactions in (1a): O4-H1w...O1 = 2.22 Å, O4...O1 = 2.942(5) Å with angle at H1w = 143°; N3-H3...O1 = 2.02 Å, N3...O1 = 2.879(5) Å with angle at H3 = 170°; O4-H2w...O3¹ = 2.04 Å, 2.828(5) Å with angle = 156° for (i) 1 - x, -y, z; Cg(N2, N3, C6-C8)...Cg(N2, N3, C6-C8)ⁱ = 3.411(2) Å. Intermolecular interactions in (1b): N3-H3...O2¹ = 1.94 Å, N3...O2¹ = 2.759(4) Å, with angle at H3 = 156° for (i) x, -1 + y, z.

- (37) Intermolecular interactions in **(2a)**: Cg(S1, N2, C6, C7, C12)···Cg-(N3, C13–C17)ⁱ = 3.574(3) Å; Cg(S2, N4, C18, C19, C24)···Cg-(N1, C1–C5)ⁱⁱ = 3.716(3) Å; Cg(N1, C1–C5)···Cg(C19–C24)ⁱ = 3.772(3) Å; Cg(N3, C13–C17)···Cg(C7–C12)ⁱⁱ = 3.641(3) Å; Cg(S3, N6, C30, C31, C36)···Cg(S4, N8, C42, C43, C48)ⁱⁱⁱ = 3.599(3) Å; Cg(N5, C25–C29)···Cg(N7, C37–C41)ⁱⁱⁱ = 3.599(3) Å; Cg(C31–C36)···Cg(C43–C48)ⁱⁱⁱ = 3.779(3) Å; Cg(S1, N2, C6, C7, C12)···Cg(N7, C37–C41)ⁱ = 3.511(3) Å; Cg(N1, C1–C5)···Cg(S4, N8, C42, C43, C48)ⁱ = 3.513(3) Å; Cg(N1, C1–C5)···Cg-(C43–C48)ⁱ = 3.777(3) Å; Cg(C7–C12)···Cg(N7, C37–C41)ⁱ = 3.739(3) Å; O9–H9···O5 = 2.10 Å, O9···O5 = 2.857(7) Å, with angle at H9 = 152° for (i) $x, 1/2 - y, -1/2 + z$, (ii) $x, 1/2 - y, 1/2 + z$, and (iii) $2 - x, 1 - y, 1 - z$. Intermolecular interactions in **(2b)**: O1–H1o···O4 = 1.58 Å, O1···O4 = 2.413(3) Å with angle at H1o = 170°; Cg(S1, N2, C6, C7, C12)···Cg(S1, N2, C6, C7, C12)ⁱ = 3.619(1) Å; Cg(S2, N4, C18, C19, C24)···Cg(S2, N4, C18, C19, C24)ⁱⁱ = 3.608(1) Å; C17–H17···O3ⁱⁱⁱ = 2.35 Å, C17···O3ⁱⁱⁱ = 3.264(4) Å with an angle at H17 = 164°; C26–H26···O4^{iv} = 2.55 Å, C26···O4^{iv} = 3.305(4) Å, with angle at H26 = 137° for (i) $-x, -y, 1 - z$, (ii) $-x, -y, 2 - z$, (iii) $-1 + x, 1 + y, z$, and (iv) $1 + x, y, z$.
- (38) Intermolecular interactions in **(3a)**: N3–H3n···O1ⁱ = 1.99 Å, N3···O1ⁱ = 2.851(5) Å with angle at H3n = 172°; N3–H3n···O2ⁱ = 2.60 Å, N3···O2ⁱ = 3.164(5) Å, with angle = 123°; Cg(N2, N3, C6–C8)···Cg(C7–C12)ⁱⁱ = 3.651(2) Å; C10–H10···O2ⁱⁱⁱ = 2.50 Å, C10···O2ⁱⁱⁱ = 3.415(5) Å with angle = 166° for (i) $x, -1 + y, z$, (ii) $-x, -y, -z$, and (iii) $-1 - x, -y, -z$. Intermolecular interactions in **(3b)**: O2–H2o···O3 = 1.58 Å, O2–H2o···O3 = 2.414(3) Å with an angle at H2o = 175°; C1–H1···O2ⁱ = 2.50 Å, C1···O2ⁱ = 3.367(3) Å with angle = 153°; N3–H3n···O4ⁱⁱ = 1.89 Å; N3···O4ⁱⁱ = 2.755(3) Å with angle = 170°; C3–H3···O4ⁱⁱ = 2.49 Å, C3···O4ⁱⁱ = 3.383(3) Å with angle = 160°; Cg(N2, N3, C6–C8)···Cg(N1, C1–C5)ⁱⁱⁱ = 3.623(1) Å for (i) $-x, 2 - y, 1 - z$, (ii) $1/2 - x, -1/2 + y, 1/2 - z$, and (iii) $1 + x, y, z$. Intermolecular interactions in **(3c)**: N3–H3n···F3ⁱ = 1.85 Å, N3···F3ⁱ = 2.719(3) Å with an angle at H3n = 178°; C1–H1···F3ⁱⁱ = 2.41 Å, C1···F3ⁱⁱ = 3.284(3) with angle = 155°; C5–H5···F2ⁱⁱⁱ = 2.22 Å, C5–H5···F2ⁱⁱⁱ = 3.094(3) Å with angle = 154°; Cg(N2, N3, C6–C8)···Cg(C7–C12)^{iv} = 3.637(2) Å; C2–H2···Cg(C7–C12)^v = 2.70 Å with angle = 138° for (i) $1/2 - x, 1/2 - y, -z$, (ii) $x, y, 1 + z$, (iii) $2 - x, 1 - y, -z$, (iv) $1/2 - x, 1/2 - y, -z$, and (v) $1/2 - x, -1/2 + y, 1/2 - z$.
- (39) Intermolecular interactions in **(4a)**: C10–H10···O1ⁱ = 2.36 Å, C10···O1ⁱ = 3.227(5) Å with an angle at H10 of 154°; Cg(N1, C1–C5)···Cg(C7–C12)ⁱⁱ = 3.969(2) Å for (i) $-1 + x, -1 + y, -1 + z$ and (ii) $-x, 1 - y, -z$. Intermolecular interactions in **(4b)**: C2–H2···O2ⁱ = 2.52 Å, C10···O1ⁱ = 3.452(4) Å with an angle at H2 of 169°; Cg(S1, N2, C6–C8)···Cg(C7–C12)ⁱⁱ = 3.789(2) Å for (i) $1 - x, 1 - y, 2 - z$ and (ii) $-x, -y, 1 - z$.
- (40) (a) Burrell, C.; Elbjerrami, O.; Omary, M. A.; Gabbai, F. P. *J. Am. Chem. Soc.* **2005**, *127*, 12166. (b) Haneline, M. R.; Tsunoda, M.; Gabbai, F. P. *J. Am. Chem. Soc.* **2002**, *124*, 3737. (c) Omary, M. A.; Kassab, R. M.; Haneline, M. R.; Elbjerrami, O.; Gabbai, F. P. *Inorg. Chem.* **2003**, *42*, 2176. (d) Burrell, C. N.; Bodine, M. I.; Elbjerrami, O.; Reibenspies, J. H.; Omary, M. A.; Gabbai, F. P. *Inorg. Chem.* **2007**, *46*, 1388.
- (41) Ghosh, S.; Petrin, M.; Maki, A. H.; Sousa, L. R. *J. Chem. Phys.* **1987**, *87*, 4315.